Assessing dry spell and wet day frequencies over southern Africa during the summer rainy season

Wanjiru Thoithi

Supervisor: Prof. Chris Reason

This dissertation is submitted in fulfillment of the requirements for the degree of

Master of Science
in
Ocean and Atmospheric Science

Department of Oceanography
University of Cape Town

DECLARATION

I know the meaning of plagiarism and declare that all of the work in the dissertation, save for that which is properly acknowledged, is my own.

Signed by candidate	19/04/2021
Wanjiru Thoithi	Date

Table of Contents

List of Figures

List of Acronyms

CHIRPS	Climate Hazards group Infrared Precipitation with Stations
DJF	December-February
DSF	dry spell frequency
ENSO	El Niño Southern Oscillation
IOD	Indian Ocean Dipole
ITCZ	Intertropical Convergence Zone
LRB	Limpopo River Basin
LRV	Limpopo River Valley
MA	March-April
MCT	Mozambique Channel Trough
MWDF	moderate wet day frequency
OLR	outgoing longwave radiation
ON	October-November
SAM	Southern Annular Mode
SASD	South Atlantic Subtropical Dipole
SASH	South Atlantic Subtropical High
SICZ	South Indian Convergence Zone
SIOD	Subtropical Indian Ocean Dipole
SST	sea surface temperature
SWIO	southwest Indian Ocean
TTT	Tropical Temperate Trough

Acknowledgments

I would like to thank my supervisor, Prof. Chris Reason for his guidance, continuous support and incredible patience during the course of my degree. I would also like to thank Dr. Ross Blamey. Together, Prof. Reason and Dr. Blamey, with their extensive knowledge and skill, helped me by answering technical and theoretical questions and providing me with great research tips.

I am also grateful to the following for their support and words of encouragement:

Ocean and atmospheric science students.

The Ocean Womxn cohort and PIs, led by Dr. Katye Altieri.

My family and friends, with special thanks to my mother.

I would like to express my gratitude to the Alliance for Collaboration on Climate and Earth Systems Science (ACCESS), National Research Foundation (NRF) and UCT Advancing Womxn Fellowship for funding my Masters study.

Finally, I am thankful for the enfolding guidance of the Almighty.

Abstract

Rainfall over southern Africa experiences substantial temporal and spatial variability which heavily impacts poor rural populations in the region that rely on rainfed agriculture for their livelihoods. Instead of totals, seasonal rainfall is better characterised by wet and dry events occurring within rainy seasons as knowledge of the frequency of such events is able to inform agricultural activity. Dry spells (pentads having $<$5 mm) and moderate wet days (10-30 mm) over southern Africa were assessed using high resolution (0.05°) Climate Hazards group Infrared Precipitation with Stations (CHIRPS) datasets over the period 1981/82-2018/19 during October-November (ON), December-February (DJF) and March-April (MA) using climatology, intensity-frequency and trend analysis. Correlations with SST over the tropical southeast Atlantic and climate modes namely, El Niño Southern Oscillation (ENSO), the Subtropical Indian Ocean Dipole (SIOD) and Southern Annular Mode (SAM) were computed. These, together with regressed atmospheric and SST fields were used to identify possible mechanisms for changes in dry spell and moderate wet day frequencies during austral summer.

Two strong gradients in dry spell frequency were found to be present during DJF, one diagonal along the western margins of the Kalahari desert and the other meridional, lying across 20-24°S. Topographic influences on rainfall were observed near the Drakensberg and Chimanimani mountains, Mulanje massif and Madagascan highlands where dry spell frequency (DSF) (moderate wet day frequency (MWDF)) tended to be relatively lower (higher). A region which frequently experienced half of the season as dry was identified lying across 22-24°S (18-25°S) during DJF (MA), with a core in the central Limpopo River Valley where 85-100% (100%) of the seasons were dry for half the season. DSF and MWDF trends indicated that drying has occurred over central South Africa during ON whereas decreasing DSF and increasing MWDF trends pointed to a weakening diagonal and meridional gradient during DJF. Additionally, increasing MWDF trends over important agricultural areas have occurred during DJF. Trends over central South Africa, part of the diagonal gradient, were associated with changes in ENSO, SAM, the Botswana High and SST in the SE Atlantic whereas those in the western Botswana region, part of the meridional gradient, were associated with those in the SIOD, Mozambique Channel Trough and Mascarene High and SST in the eastern and western Pacific.

1 Introduction

Southern African rainfall is characterised by temporal variability on scales ranging from intraseasonal to decadal and longer (Tyson et al., 2002; Reason and Rouault, 2002; Chikoore and Jury, 2010), as well as variation in spatial distribution (Taljaard, 1986). This variability is driven by an array of climatic processes interacting at different temporal and spatial scales, making the region prone to extreme rainfall events that lead to drought and flooding (Fauchereau et al., 2003). It is a great matter of concern that widespread changes in the mean state, seasonality and variability of rainfall are expected to occur in the future (IPCC, 2013). Southern Africa, for example, hosts large arid and semi arid ecosystems which are more sensitive to shifts in rainfall patterns (Weltzin et al., 2003; Huang et al., 2016). Changes in rainfall patterns also have impacts on human lives, especially where food production systems are concerned.

Food security is a function of complex variables whose nature ranges from physical to economic and is considered to be a global developmental priority (Conceição et al., 2016). One major determinant of achieving food security is food availability, which is influenced to a great degree by agricultural production. Southern Africa has a large food insecure population for the following reasons. High poverty and population growth rates predispose the majority of its inhabitants to food insecurity (Lipper et al., 2014; Conceição et al., 2016). Additionally, most food production in the region is dependent on rainfed agriculture, thus extreme rainfall events and projected shifts in their frequency pose a major threat to food production (Ziervogel et al., 2006).

Hydrometeorological extremes such as droughts and floods are known to be disruptive to food production systems (Steenwerth et al., 2014). The higher their frequency and intensity, the more difficult it is for agricultural systems to recover or build resilience (Thornton et al., 2014). Southern Africa has experienced a number of extreme events in the recent past which have adversely affected food production. The 2015/2016 drought led to a food security crisis in Madagascar, Malawi, Mozambique and Zimbabwe due to a decrease in food production (ReliefWeb, 2015). Ongoing persistent dry conditions (2018-2020) have resulted in high levels of food insecurity across many southern African countries (ReliefWeb, 2018). Flooding has also contributed to widespread crop damage. In 2017, above average seasonal rainfall deluged many parts of the region (ReliefWeb, 2017).

Climate-smart agriculture (CSA) is an approach to agriculture that comprises multiple strategies to transform agriculture towards sustainability and attaining food security in the face of climate change (Steenwerth et al., 2014; Lipper et al., 2014; Sullivan et al., 2012). It requires the engagement of multiple stakeholders, including researchers, farmers and policymakers to achieve its ends. Filling in of knowledge gaps is fundamental to the formulation of science-based policies. One identified need in research is the further spatio-temporal study of climate trends since this will help stakeholders understand the potential impacts of changes in climate means and extremes on food security (Steenwerth et al., 2014; Ziervogel et al., 2006).

Precipitation is one of the more crucial variables to measure with respect to agricultural systems (Ziervogel et al., 2006). Many studies have undertaken the analysis of rainfall using seasonal totals. While this is important as a first step to determining links between rainfall and various climatic processes, as well as trying to predict seasonal rainfall totals (Mutai and Ward, 2000), rainy seasons tend to be made up of a combination of wet and dry spells occurring after and before defined onset and cessation dates that directly influence human activities. Therefore, rainfall characteristics provide more useful information about rainfall to user groups and stakeholders such as farmers and water resource managers than seasonal totals do. It is changes in rainfall characteristics that have been associated with breakdowns in agricultural productivity. For example, increased dry spell duration has been associated with drought and a decrease in growing period duration (Tadross et al., 2005, 2009). Furthermore, while the amount of rainfall may remain relatively the same over time, changes occurring in the distribution of wet and dry events within the season may have severe implications for agriculture (Pohl et al., 2017).

With all this in mind, this work aims to analyse rainfall characteristics, namely dry spell and wet day frequency over southern Africa during austral summer. In doing so, it will identify patterns in their spatial distribution and regions more susceptible to their high occurrence. Additionally, in performing trend analysis of dry spell and wet day characteristics, it will identify regions of significant change and potential mechanisms of change.

2 Literature review

2.1 Overview of southern African rainfall

The subcontinent of southern Africa can be defined as Africa south of the equator although some authors take it to mean the region south of 10°S or even 15°S (Lyon and Mason, 2007). Southern Africa's topography comprises of a plateau in the interior separated from a thin coastal plain strip by narrow mountain ranges in the south (Moore et al., 2009; Reason, 2017). Surrounded by the South Atlantic to the west and the South Indian Ocean to the east, southern Africa's unique geographic location makes it subject to a mix of tropical, subtropical and midlatitude climatic influences (Tyson and Preston-Whyte, 2000). With the exception of most of Tanzania (bimodal regime), the southwestern part of South Africa (austral winter) and the south coast of South Africa (all year), the greater part of southern Africa receives most of its rainfall during austral summer (Taljaard, 1986; Nicholson, 2000). Depending on the topic studied, the summer rainy season can be defined as September to April (Taljaard, 1986), December to April (Fauchereau et al., 2003) or October to March (Lyon and Mason, 2007). According to Lyon and Mason (2007), between 40% to more than 80% of summer rainfall in southern Africa is received over the period December-March. Most sub-regions in southern Africa have a rainfall maximum in January (Nicholson, 2000).

2.2 Seasonal rainfall

Cloud bands extending across southern Africa are predominantly responsible for producing rainfall over the region during austral summer (Harrison, 1984; Usman and Reason, 2004; Reason et al., 2005; Hart et al., 2013; Ratna et al., 2013). Referred to as Tropical Temperate Troughs (TTTs), the northwest-southeast oriented cloudbands involve tropical-extratropical interactions occurring over southern Africa and neighbouring oceans (Hart et al., 2010; Macron et al., 2014). These interactions involve the transport of heat and moisture away from the tropics to the midlatitudes (Hart et al., 2010). On average, TTTs contribute significantly to summer rainfall in subtropical southern Africa and exhibit substantial intraseasonal and interannual variability (Hart et al., 2010, 2018; Macron et al., 2014). The aggregate of the synoptic scale TTT events over the summer essentially forms the South Indian Convergence Zone (SICZ)

(Hart et al., 2010, 2018; Macron et al., 2014; Dedekind et al., 2016) which in contrast its counterparts, the South Pacific and South Atlantic Convergence Zones, is less coherent or anchored to a particular location. The development of TTTs requires the presence of a easterly disturbance in the lower troposphere of the tropics and a westerly wave with an associated front passing south of South Africa. The movement of the upper-tropospheric westerly trough over southern Africa triggers cloud band formation. (Hart et al., 2010; Macron et al., 2014).

The SICZ is a northwest-southeast slanted region extending from the southeast coast of southern Africa to the southwest Indian Ocean and may be identified in seasonal averages of convective clouds and precipitation (Cook, 2000; Nicholson, 2000; Fauchereau et al., 2009). It is present over parts of southern Africa during austral summer but is variable in its distinctness from year to year (Cook, 2000; Fauchereau et al., 2009; Hart et al., 2010). According to Cook (2000), the SICZ is distinct from the Intertropical Convergence Zone (ITCZ). The former contributes to southern African rainfall as it is linked to the development of TTT and cloud bands over southern Africa. (Fauchereau et al., 2009; Dedekind et al., 2016).

One of the seasonal circulation systems contributing to austral summer rainfall is the ITCZ, a narrow region near the equator which forms the meeting point of the northeast and southeast trade winds (Grodsky and Carton, 2003; Yan, 2005; Schneider et al., 2014). The convergence of winds forces moist air upward which leads to the formation of cumulus clouds and the occurrence of precipitation. Over West Africa, the ITCZ is the region where the northeasterly Harmattan winds and the southwesterly monsoon meet (Nicholson, 2018). Over eastern Africa, it is characterised by pronounced seasonal migration to the north and south of the equator along with the development of the South West and North East monsoons during austral winter and summer, respectively (Taljaard, 1986). Over the Atlantic seaboard of Africa, the ITCZ tends to remain north of the equator throughout the year (Reason et al., 2006). During austral winter, the average position of the ITCZ lies between 18°and 20°N whereas in austral summer, the ITCZ migrates southward across Tanzania into northern Madagascar, northern Mozambique, southern Malawi and southern Zambia, bringing rainfall into southern Africa (Goddard and Graham, 1999; Nicholson, 2000). The ITCZ is well known to influence global tropical climate (Yan, 2005). Convection associated with this convergence zone contributes to barotropic and baroclinic instability which, according to Ferreira and Schubert

(1997), may cause the ITCZ to break down into tropical disturbances and result in tropical cyclogenesis over the tropical South Indian Ocean. Convective circulation associated with the ITCZ is also known to produce tropical thunderstorms and significant precipitation over southern Africa (Collier and Hughes, 2011).

Although the ITCZ has been described as a region of maximum precipitation (Schneider et al., 2014), Nicholson (2018) notes that the location of the ITCZ does not necessarily coincide with that of maximum precipitation. For example, in West Africa, the zone of maximum rainfall and that of wind convergence are decoupled (Nicholson, 2018). The ITCZ and the rainfall maximum are almost co-located over southern Africa during austral summer (Janowiak, 1988). Thus, the ITCZ contributes significantly to seasonal rainfall over the region (Dedekind et al., 2016).

2.3 Interannual variability

The interannual variability of rainfall over southern Africa is modulated by large-scale climate anomalies such as the Subtropical Indian Ocean Dipole (SIOD) (Reason, 2001), South Atlantic Subtropical Dipole (SASD) (Vigaud et al., 2009) and El Niño Southern Oscillation (ENSO) (Nicholson and Kim, 1997; Reason and Jagadheesha, 2005). The SIOD is characterised by opposing sea surface temperature (SST) anomalies in the western and eastern parts of the subtropical South Indian Ocean and is outlined by Behera and Yamagata (2001) as follows. During the positive phase of SIOD, warm SST anomalies mark the southwest Indian Ocean (SWIO), just south of Madagascar and cold ones, the southeastern Indian Ocean off Australia. These anomalies are associated with shifts in the position and strength of the subtropical high which according to Hermes and Reason (2005) may be brought about by changes in southern hemisphere midlatitude circulation patterns. Anomalies in the subtropical high lead to changes in winds over the South Indian Ocean, which then result in modulations in heat transport and fluxes that generate SST anomalies in the southwest and southeast Indian Ocean. In its positive phase, southeasterlies off the west coast of Australia tend to be stronger than usual, resulting in increased evaporation over the south eastern Indian Ocean and cooling off the coast of Australia (Behera and Yamagata, 2001). At the same time, a weakening in the midlatitude westerlies, contributes to relative decrease in latent heat loss over the SWIO and warm SST anomalies.

The SIOD typically begins its evolution in late austral spring, reaches its peak around January and decays by May (Suzuki et al., 2004). Its variability has been shown to be related to precipitation anomalies over southern Africa during austral summer, the season to which it is locked (Behera and Yamagata, 2001; Reason, 2001, 2002; Suzuki et al., 2004). Enhanced southeasterlies during positive events transport moist air towards southeastern and southcentral Africa where low-level convergence results in postive rainfall anomalies. Opposite anomalies occur during negative SIOD events due to divergence of dry air over southeastern Africa (Reason, 2002). However, Suzuki et al. (2004) note that the relationship between southeastern African rainfall and the SIOD is nonlinear and that rainfall is not highly sensitive to SIOD-related SST anomalies. Morioka et al. (2012) reported that positive SIOD events only result in positive rainfall anomalies over southern Africa if they co-occur with a positive SASD event. Otherwise, significant rainfall anomalies can only be found over Angola and Madagascar.

The South Atlantic Ocean is one of the major sources of moisture for southern African precipitation. Analogous to the SIOD, the SASD is the dominant mode of SST variability over the South Atlantic and has been shown to contribute to the interannual variability of rainfall over southern Africa during austral summer (Vigaud et al., 2009; Morioka et al., 2012; Wainer et al., 2014). Consisting of a dipole-like structure of SST anomalies in the South Atlantic Ocean (Morioka et al., 2011), the SASD is associated with changes in the position and strength of the South Atlantic Subtropical High (SASH) (Wainer et al., 2014). During its positive phase, the increase in strength and southward movement of the SASH suppresses (increases) the latent heat flux which causes a mixed layer depth anomaly to develop. The thinner (thicker) mixed layer in the positive (negative) pole leads to enhanced (reduced) warming and positive (negative) SST anomalies (Morioka et al., 2011). The reverse occurs for the negative phase of the SASD. Referring to the mode of variability associated with changes in the strength and position of the South Atlantic Anticyclone, the South Atlantic Midlatitude Mode, Vigaud et al. (2009) found that the negative phase, linked with the southward migration of the South Atlantic Anticyclone, is associated with reduced moisture advection over southern Africa and changes in regional circulation that lead to postive rainfall anomalies. Similarly, Morioka et al. (2012), found that during positive SASD phases associated with the strengthening and southward migration of the SASH, there are above average rainfall anomalies over southern Africa. Though the phases are termed differently, both studies associate the southward migration of SASH with positive rainfall anomalies

over southern Africa.

ENSO is well known to impact climate globally on interannual time scales. Over southern (East) Africa, it's influence is greatest during January-March (October-December) (Nicholson and Kim, 1997; Reason et al., 2000) with typically drier (wetter) than average conditions occurring during El Niño (La Niña). El Niño and La Niña years are marked by shifts in the general circulation over southern Africa. During El Niño, there tend to be continental high pressure anomalies and a stronger Botswana High/weaker Angola Low (Driver and Reason, 2017), conditions unfavourable for deep convection (Lyon and Mason, 2007; Meque and Abiodun, 2015). During La Niña, there tend to be anomalous low pressure anomalies over the region which promote convection and enhance precipitation over southern Africa (Reason et al., 2000; Lyon and Mason, 2007).

The relationship between ENSO and precipitation is complex and non-linear (Hoerling et al., 2001; Reason and Jagadheesha, 2005; Meque and Abiodun, 2015). Rainfall anomalies received during particular ENSO events are strongly influenced by whether or not ENSO impacts significantly on key regional circulation systems such as the Angola Low or the Botswana High (Reason, 2016; Driver and Reason, 2017; Blamey et al., 2018). Average summer rainfall amounts have been documented during El Niño and La Niña years (Landman and Beraki, 2012). The strong El Nino of 1997/98 is one such event that was not marked by dry conditions over southern Africa but by near and in some areas, above average rainfall. In a comparative study of El Niño and La Niña related anomalies, Reason and Jagadheesha (2005) found that the 1997/98 El Niño was associated with increased moisture flux from the southeast Atlantic (off the coast of Angola) and a stronger Angola Low, all of which acted to oppose the typical El Niño signal observed in historical teleconnection patterns. Similarly, Lyon and Mason (2007) found that the 1997/98 El Niño event was associated with a relatively intensified Angola Low and increased moisture flux from the southern African interior and the tropical Indian Ocean.

A phenomenon similar to ENSO which involves the occurrence of warm and cold events in the tropical southeast Atlantic (Shannon et al., 1986; Florenchie et al., 2004) has been shown to impact rainfall over coastal Angola and Namibia and in some instances, parts of the southern African interior (Rouault et al., 2003; Reason and Smart, 2015). During warm events, due to changes in the trade winds over the western equatorial Atlantic, warm equatorial Atlantic water propagates southward along the west coast of southern Africa where the

upwelling of cool water typically occurs (Shannon et al., 1986). This occurrence has been distinguished from typical warm ENSO events as it does not necessarily coincide with El Niño events (Florenchie et al., 2003). Southeast (SE) Atlantic SST events modulate southern African rainfall mostly during austral summer since the impact of warm SST anomalies on atmospheric instability is greater during the season of highest mean SST (Rouault et al., 2003). Warm events tend to be associated with above average rainfall anomalies over the coast of Angola and northern Namibia, brought about by increased easterly moisture flux from the western tropical Indian Ocean and westerly flux from the tropical south east Atlantic (Rouault et al., 2003; Reason and Smart, 2015). Additionally, a weakened Botswana High provides suitable conditions for deep convection and the formation of rainfall (Reason and Smart, 2015).

2.4 Regional circulation features

Regional circulation features modulate the interannual variability of rainfall over southern Africa. Some of these include the Angola Low, Botswana High and Mozambique Channel Trough (MCT). The Angola Low is a semi-permanent cyclonic system located over the Bié plateau in central Angola (Mulenga et al., 2003; Cook et al., 2004; Munday and Washington, 2017; Howard and Washington, 2018; Crétat et al., 2019). According to (Munday and Washington, 2017), this low pressure system forms in austral summer, developing from October through March. During austral spring it is present as a heat low which forms due to surface heating. Later on, the structure of the Angola low transforms and resembles that of a tropical trough. The two phases have been found to have different dynamics and relationships with ENSO and southern African precipitation. Notably, only the Angola tropical low phase modulates ENSO's impact on southern African precipitation (Howard and Washington, 2018). The strengthening of the Angola Low has been associated with changes in circulation namely, increased local convection and moisture flux from the southeast Atlantic Ocean and the penetration of moist northeasterlies from the tropical western Indian Ocean further into the subcontinent (Munday and Washington, 2017). These changes act to increase low level convergence over Angola and the neighbouring south east region. When westerly waves pass over this region, the formation of TTTs may be triggered, bringing about rainfall across many parts of southern Africa (Munday and Washington, 2017; Macron et al., 2014; Hart et al., 2010).

Several studies have detailed the relationship between the Angola Low and rainfall over various regions across southern Africa. During dry ENSO summers, Mulenga et al. (2003) found that a weakened Angola Low provided unsuitable conditions for the formation of cloud bands over southern Africa. Cook et al. (2004) found that the Angola low tended to be strengthened during early and late wet summers whereas it tended to be weakened during early and late dry summers. The Angola low has also been linked to a significant proportion of variability between climate models in simulating rainfall during austral summer over southern Africa (Munday and Washington, 2017). Crétat et al. (2019) found that the Angola Low has several main states which correspond to various shifts in the spatial and temporal distribution of rainfall over southern Africa. Only a few phases were found to have a significant relationship with ENSO. These studies show that the strength and position of the Angola Low play an important role in influencing the distribution of rainfall across southern Africa and during the austral summer rainfall season.

Like the Angola Low, the Botswana High has been found to play an important role in influencing rainfall over southern Africa (Hart et al., 2010; Reason, 2016; Driver and Reason, 2017; Blamey et al., 2018). It is a semi-permanent mid-level anticyclone which develops from austral spring through summer. It forms in response to condensational heating over the tropical region of high precipitation over Africa (in Congo) and occurs to the south west of this high precipitation region (Reason, 2016). Forming in August, the Botswana High migrates southwards through austral spring and summer. Its location is linked to the southward migration of the ITCZ and the region of highest precipitation according to Driver and Reason (2017) who outlined the evolution of the Botswana High through austral spring and summer as follows. In the month of July the tropical region of high precipitation lies in the northern Congo basin. The Botswana High develops over the region covering southern Angola, northern Namibia and northwestern Botswana, south west of the high precipitation area over the Congo basin. It grows in intensity and shifts southwards, following the southward migration of the ITCZ over southern Africa, reaching its maximum intensity in February. Thereafter, it weakens and begins to move northwards while reaching its maximum zonal extent in March, extending from the South Atlantic Convergence Zone to the western Indian Ocean.

According to Driver and Reason (2017), the relationship between the Botswana High and rainfall over southern Africa is strongest from January to March. They correlated rainfall over the main summer rainfall region of southern Africa and

geopotential height at 500 hPa and found there to be fairly strong negative correlation values over the region of the Botswana High core. Generally, an intensified (weakened) Botswana High is linked to reduced (increased) rainfall over the region. They also found that neutral ENSO years during which the Botswana High had negative anomalies were associated with a widespread cyclonic anomaly, increased uplift over southern Africa and increased moisture transport from the southwest Indian Ocean, conditions favourable for the formation of TTTs. Approximately the opposite was found for summers with negative anomalies. The Botswana High has been reported to have a significant relationship with ENSO. There is a high positive correlation between the Botswana High and the Niño 3.4 index, however, this relationship is not linear. (Driver and Reason, 2017; Blamey et al., 2018). Blamey et al. (2018) found that during the 2015/2016 El Niño,the Botswana High, along with the Angola Low and South Indian Ocean High played an important role in modulating the spatial and temporal distribution of rainfall across southern Africa. The Botswana High in particular was found to be stronger compared to previous El Niño events, its subsidence preventing the formation of rainfall rand resulting in unprecedented widespread dry conditions.

The role of the MCT in influencing southern African rainfall has received relatively less attention. This cyclonic circulation is present over the central and southern Mozambique Channel during austral summer and develops due to the dynamical adjustment of easterlies flowing over Madagascar's high topography (Barimalala et al., 2018, 2020). According to Barimalala et al. (2018), the MCT is present from December to April but is at peak strength during February, thereafter gradually weakening. The cyclonic anomaly associated with a stronger MCT results in the formation of oceanic cloud bands which bring about above average rainfall over the SWIO ocean and below average over the southern African subcontinent. A weaker MCT increases easterly moisture transport and tends to be associated with increased rainfall over southern Africa and a decrease over northern Mozambique, Madagascar and the Mozambique channel.

The relationship between regional circulation features and rainfall over southern Africa is complex due to the interplay with ENSO and possibly with other modes of variability, as shown in the studies above The intensity of regional circulation features can modify ENSO impacts on southern African rainfall (Reason and Jagadheesha, 2005). Additionally ENSO-related signals can impact regional circulation features which in turn influence rainfall over the region

(Blamey et al., 2018). Regional circulation features also modulate rainfall distribution during neutral ENSO events (Driver and Reason, 2017). Knowledge of the variability of regional circulation features is important for providing key insights into rainfall variability over southern Africa. It may also reveal potential for rainfall predictability through monitoring of atmospheric circulation and in doing so, improve seasonal forecasting of rainfall.

2.5 Intraseasonal timescales

In the past, climate research has had a tendency to focus on seasonal rainfall totals and their anomalies (Mutai and Ward, 2000; Hachigonta and Reason, 2006). Analysing seasonal rainfall is important as a first step in determining links between rainfall and various climate processes, as well as trying to predict seasonal rainfall totals (Mutai and Ward, 2000; Reason et al., 2005). However, rainy seasons tend to be made up of a combination of wet and dry spells occurring after and before defined onset and cessation dates. Thus stakeholders such as farmers and water resource managers require more meaningful information on likely rainy season characteristics (Reason et al., 2005). Research of the variability of rainfall characteristics and associated circulation anomalies may provide information on the predictability of these parameters and their likely patterns.

A number of studies have examined rainfall characteristics over various subregions of tropical (Kijazi and Reason, 2005; Mapande and Reason, 2005) and subtropical southern Africa (Cook et al., 2004; Tennant and Hewitson, 2002; Usman and Reason, 2004; Reason et al., 2005; Hachigonta and Reason, 2006; Hachigonta et al., 2008; Tadross et al., 2009; Randriamahefasoa and Reason, 2017). Although studies such as these provide useful information about rainfall characteristics, when carried out at a subnational scale may miss out on large scale rainfall patterns and the potential drivers and mechanisms behind variability. Those carrying out regional assessments of rainfall characteristics by averaging them over very large areas do not account for spatial variation. Studies that investigate rainfall characteristics over much larger areas at every grid point include Usman and Reason (2004) (southern Africa), Dunning et al. (2016) and Dunning et al. (2018) (Africa).

Of particular interest to this dissertation is work done by Usman and Reason (2004) who examined the distribution, variability and trends of dry spell fre-

quencies over southern Africa south of the equator during December-February (DJF). They found that dry spell frequency tended to be higher (lower) during El Ninõ (La Niña) for most of southern Africa. Additionally, the occurrence of dry spell frequencies was linked to changes in the shape and position of TTTs over the region and the SWIO. A preferred zone of dry spell frequency occurrence was found across 20-25°S. This region stood out as one with high susceptibility to drought and was termed the drought corridor.

While Usman and Reason (2004) provided a useful assessment of spatial and temporal patterns in dry spell frequency over southern Africa, they used low resolution data (2.5°) over the period 1979-2002. High resolution (0.05°) data is now available over a longer time period (1981-present), which is more suitable for composite and interannual variability analyses and capturing topographic influences on rainfall. Dry conditions have extensively been studied over southern Africa, which is predominantly semiarid. However, studying rainfall events that lead to both dry and wet conditions paints a more complete picture of southern African rainfall (Washington and Preston, 2006). With this in mind, this study aims to assess the distribution of dry spell and wet day frequencies over southern Africa south of 6°S during three seasons namely, October-November (ON), DJF and March-April (MA)

2.6 Objectives

In assessing dry spell and wet day frequencies over southern Africa, this study has the objective to identify:

i spatial patterns in dry spell and wet day frequencies over southern Africa by creating climatologies.

ii regions more susceptible to high dry spell and wet day occurrence through intensity-frequency map analysis

iii regions of significant trends by computing trends in dry spells and wet day frequencies.

iv potential mechanisms of change in rainfall characteristics by performing regressions and correlations with climate modes and atmospheric and SST fields.

3 Data and methods

Dry spell and wet day characteristics

The parameters dry spells and moderate wet days were selected for their agricultural relevance in maize growing, a major source of income for poor rural populations of southern Africa. These characteristics provide more useful information about rainfall with regard to germination and growth phases than seasonal totals do to user groups and stakeholders such as farmers and water resource managers. Dry spells were taken to be pentads (5-day periods) having less than 5 mm of rainfall, a definition which has been used by Usman and Reason (2004) and Reason et al. (2005). Dry days are defined as those receiving $<$1 mm of rainfall (Winsemius et al., 2014), therefore a pentad with less than 5 mm represents an extended period of dry conditions which could disrupt crop growth if occurring at a high frequency.

Moderate wet days were taken to be those containing 10-30 mm of rainfall. This definition was considered suitable since it takes into account a number factors. Sufficient rainfall during the germination and growth phase of maize is crucial for the success of the crop. Rain is unlikely to have an even distribution throughout the season thus wet days having higher rainfall (compared to the 2 mm lower threshold of wet days (Tadross et al., 2009)) are more likely to contribute to the accumulated amount of rainfall needed for each growing phase. Additionally, soil evaporation is high during the germination phase and sufficient water is required to bring top soil to field capacity (Raes et al., 2004). The upper threshold of 30 mm of rainfall (Randriamahefasoa and Reason, 2017) was selected because heavy rainy days are undesirable for crop growing and may reduce yields due to water logging, soil erosion and nutrient leaching (Phillips et al., 1998; Tadross et al., 2007; Munodawafa, 2012).

Seasonal rainfall

Southern Africa south of about 6°S has been shown to have a predominantly annual rainfall regime (Dunning et al., 2016). According to Fig. 1, the season of the highest rainfall corresponding to the largest percentage area of southern Africa is DJF (46%), followed by JFM (31%). Therefore, analysis of dry spells and moderate wet days was done with a focus on the core of the rainy season,

DJF. Attention was also given to the transition seasons of ON and MA during which the onset and withdrawal of the rains typically occurs.

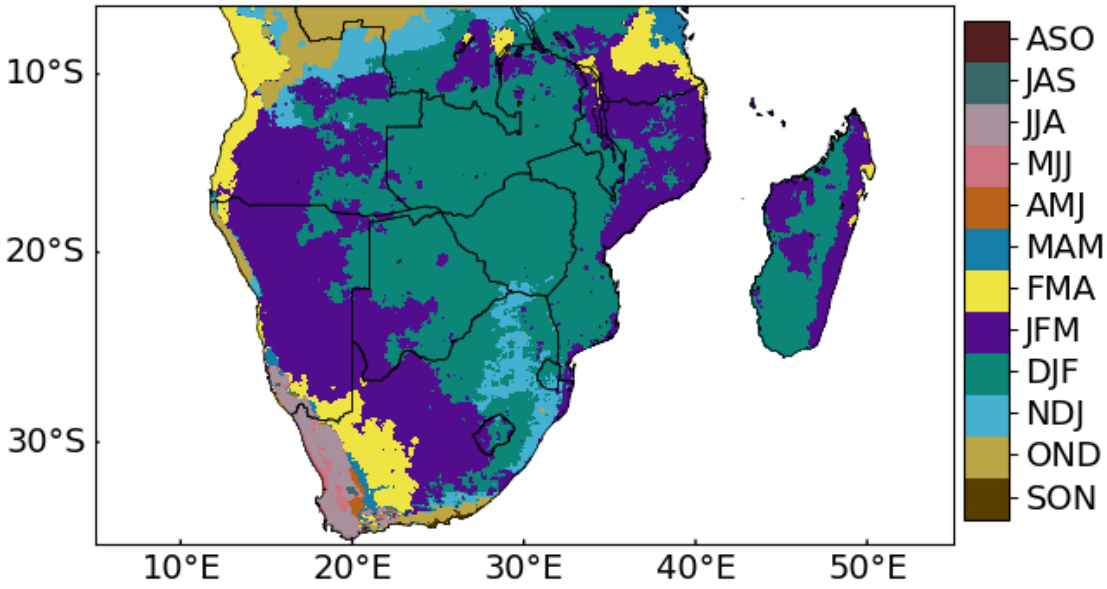

Figure 1: Map showing the season of the highest mean seasonal total over the period 1981/82-2018/2019 using a 0.05° monthly Climate Hazards group Infrared Precipitation with Stations (CHIRPS) dataset.

It should be noted that an assessment of rainfall characteristics was not carried out using climate models for the following reasons. Current models use a relatively coarse resolution compared to that required to capture local topographic influences on rainfall and other rainfall spatial patterns. Models also experience challenges in convective parameterisation over southern Africa, and consequently in the representation of southern Africa's main rain-bearing systems which are convective in nature. This study requires an observational precipitation product with sufficient area coverage, high temporal resolution (daily) and high spatial resolution compared to 2.5°, as used in Usman and Reason (2004). Several satellite-derived rainfall datasets are now available for sufficiently long periods, some of which include a global dataset with a resolution of 0.25° from Precipitation Estimation from Remotely Sensed Information using Artificial Neural Networks- Climate Data Record (PERSIANN-CDR) (Ashouri et al., 2015) and those from the Tropical Rainfall Measuring Mission (TRMM), which have near-global coverage and a resolution of 0.25° (Huffman et al., 2007). High resolution (0.05°) quasi-global datasets from CHIRPS (Funk et al., 2015) were chosen over the above products for following reasons. They are available over a longer period than those from TRMM, which date

back to 1998 (CHIRPS however incorporates TRMM data after 1998). While CHIRPS and PERSIANN datasets are available over a comparable time period (1981 to near-present and 1983 to near-present, respectively), CHIRPS has been shown to provide reliable rainfall estimates within parts of southern Africa (Muthoni et al., 2019) and has applications in drought monitoring across Africa (Shukla et al., 2017). Thus, high resolution (0.05 °) CHIRPS pentad and daily datasets were used to generate time series of dry spells and moderate wet days, repsectively, for the period 1981/82 - 2018/19 during ON, DJF and MA over southern Africa south of 6°S. Time series were then averaged to create climatologies of dry spell and moderate wet day frequencies over the period 1981/82-2018/19.

Intensity-frequency is a statistic used by Usman and Reason (2004) to determine the susceptibility of a region to drought. In this study, intensity-frequency maps were plotted to show the percentage number of seasons having 9 or more dry spells (the duration of half the season) and those having at least 20 moderate wet days during the main summer season (DJF). For the transition seasons of ON and MA, maps display the percentage number of seasons having 6 or more dry spells and 10 or more moderate wet days. Trends in moderate wet day frequency (MWDF) and dry spell frequency (DSF) over the period 1981/82-2018/19 were computed using the Theil-Sen slope estimator (Theil, 1950; Sen, 1968) and Mann-Kendall test (Mann, 1945; Kendall, 1975). These non-parametric methods are robust and thus not sensitive to outliers.

Relationships with modes of climate variability were evaluated by computing the Pearson correlation coefficient between DSF and MWDF time series and climate indices namely, Niño 3.4 index using the Hadley Centre Sea Ice and SST version 1.1 dataset (HadISST1) (Rayner et al., 2003) obtained from http://climexp.knmi.nl/data/ihadisst1_nino3.4a.dat, Southern Annular Mode (SAM) Marshall index (Marshall, 2003) obtained from https://legacy.bas.ac.uk/met/gjma/sam.html and SIOD index (Behera and Yamagata, 2001) obtained from http://www.jamstec.go.jp/virtualearth/data/SINTEX/SINTEX_SIOD.csv. DSF and MWDF over southern Africa were also correlated with an index of SST anomalies over the SE Atlantic (8°E to the coast, 10–20°S, as in Rouault et al. (2009)) to determine the relationship with tropical SE Atlantic events. SST data was obtained from the National Oceanic and Atmospheric Administration's (NOAA's) Optimal Interpolation SST analysis, version 2 (OISSTV2) which has a resolution of 0.25° (Reynolds et al., 2002).

To investigate the potential mechanisms and drivers behind changes in the

occurrence of rainfall characteristics during the main rainy season, DSF and MWDF were averaged over smaller grid-boxes of nearly equal horizontal resolution (1.95°x 2.5°). Linear regressions were performed with various atmospheric fields and SST during DJF for the period 1981/82-2018/19. Monthly geopotential height at 500 hPa was obtained from European Centre for Medium-Range Weather Forecasts Reanalysis v5 (ERA5)(Hersbach et al., 2020). The ERA5 atmospheric reanalysis is a replacement for European Centre for Medium-Range Weather Forecasts Reanalysis-Interim (ERA-Interim) (Dee et al., 2011) and in its production improves on ERA-Interim through advancements in modeling and the assimilation of data. ERA5 better represents convective activity and other atmosopheric features (Hoffmann et al., 2019) since it uses a higher spatial resolution (0.25°) compared to ERA-Interim (0.75°) and the National Centers for Environmental Prediction-Department of Energy (NCEP-DOE) Reanalysis II (2.5°) (Kanamitsu et al., 2002). Moisture flux (Q) was computed using horizontal wind components and specific humidity at 850 hPa from ERA5 according to the following equation:

$$\vec{Q} = q\vec{V_h}$$

where q is specific humidity and V_h is horizontal wind.

Regressions were also performed with outgoing longwave radiation (OLR) data from University of Maryland's OLR Climate Data Record which has a horizontal resolution of 2.5° and omega at 500 hPa from ERA5 (0.25°).

4 Results

The interpretation of the following results will be given in the Discussion section. The most important results are in production in Thoithi, W., Blamey, R. C. and Reason, C. J. C. 2021. Dry spells, wet days and their trends across southern Africa during the summer rainy season. *Geophysical Research Letters*. doi:https://doi.org/10.1029/2020GL091041.

4.1 Dry spell frequency

Mean dry spell frequency

Fig. 2a shows the distribution of dry spell frequency across southern Africa during ON, taken here to be the transition season into austral summer. Two gradients in dry spell frequency were observed over the region. The first is diagonal, stretching across southwestern Angola, Namibia and western South Africa. This area on average had between 8 and 12 dry spells per season with the maximum frequency (12 dry spells) present at the westernmost extent of the gradient. The second gradient was observed centered along a NW-SE axis, extending from northern Angola and southern DR Congo to southern Angola and Zambia. On average, the number of dry spells across this gradient ranged from 1 to 8. High dry spell frequency (9-12) was found over Tanzania, northern Mozambique and the western coast of Madagascar. Eastern South Africa notably had relatively low dry spell frequencies of below 5, a contrast to the western part of the country where on average, all twelve pentads were experienced as dry.

During DJF, the main rainy season, there were fairly large areas with fewer than 3 dry spells on average as shown in Fig. 2b. These include the 6-18°S latitudinal band (with the exception of western Angola and eastern Tanzania), Madagascar and eastern South Africa, roughly along the Drakensberg mountain range. On average, less than a third of the eighteen-pentad season was experienced as dry over these regions. As with ON, two dry spell frequency gradients were observed over southern Africa during DJF. The diagonal gradient present during ON persisted through DJF, though stronger, with frequencies ranging from 7 to 18. It was found located roughly along the western margins of the Kalahari desert, extending from southwestern Angola to western South Africa. The second gradient is meridional, located across the 20-24°S band with a maximum present near the center of the Limpopo River Valley (LRV), where the borders of Zimbabwe, South Africa and Botswana meet. Mean dry spell frequencies of 11-13 were observed over this maximum.

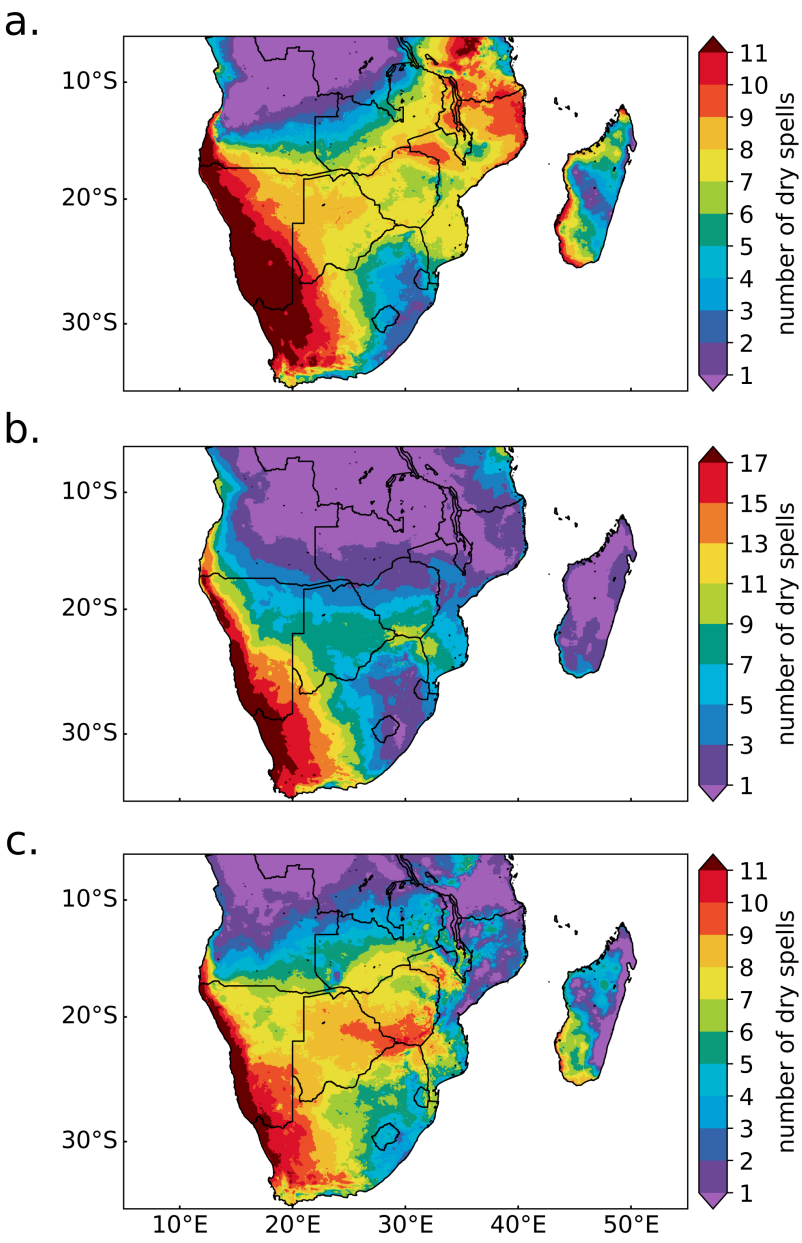

Figure 2: Dry spell frequency climatology over the period 1981/1982 – 2018/2019 during a. ON, b. DJF and c. MA.

Two gradients in dry spell frequency were present over southern Africa during the MA season, as shown by Fig. 2c. The diagonal gradient present during ON and DJF was observed in the MA climatology, extending from the southwestern tip of Angola southwards across western Namibia and western South Africa. The change in frequency across this gradient is of magnitude 4. Dry spell frequency was found to generally increase southward from about 10 to 24 °S, with a maximum centred near the Zimbabwe - South Africa border in the LRV. This region of maximum frequency experienced 11 dry spells on average.

Relatively low frequencies were observed over eastern South Africa, which experienced between 3 and 4 dry spells per season. Southwest Madagascar had markedly higher dry spell frequencies (8-11) than the rest of the island which on average had fewer than 5 dry spells.

Intensity-frequency maps

Intensity-frequency maps of Fig. 3 are indicative of the susceptibility of an area to experiencing meteorological drought. They show the percentage of the total number of seasons (38) that were dry for the duration of at least half the season (6 pentads for ON and MA, 9 pentads for DJF). Over most of southern Africa, more than 50% of ON seasons consisted of 6 or more dry spells as shown in Fig. 3a. The maximum percentage (100%) was observed over northern Tanzania and Mozambique, parts of the Zambezi near the Zimbabwe - Mozambique border and the stretch covering southwestern Angola, Namibia and western South Africa, the approximate location of the dry spell frequency gradient observed in Fig. 2a. During each of the 38 seasons studied, these areas experienced dry conditions for at least 6 pentads. Regions that stood out as having no season consisting of at least 6 dry spells ($<$3%) include central Madagascar, roughly over the central high plateau, and eastern southern Africa, near the Drakensberg mountain range. Relative minimums were observed around the border between Malawi and Mozambique, near the Mulanje Massif, and around the Chimanimani mountain range found on the border of Mozambique and Zimbabwe. Here, 25-30% of the ON seasons had 6 or more dry spells.

Fig. 3b shows the percentage of summers that were dry for at least 9 pentads (half the season). During DJF, most of southern Africa had no season with at least 9 dry spells. A maximum was observed over western southern Africa where all 38 summers consisted of 9 or more dry spells. This number decreases to 21-37 (55-97%), over the surrounding strip stretching from southwestern Angola to central South Africa. A band extending eastwards from this region to southern Mozambique (22-24°S) exists where more than 40% of the seasons had at least 9 dry spells. Herein, a maximum was found to be present in the central Limpopo River Valley where the percentage of seasons having at least 9 dry spells fell within the range of 85-100% . The significance of the latitudinal band and its core will be explained in the Discussion section.

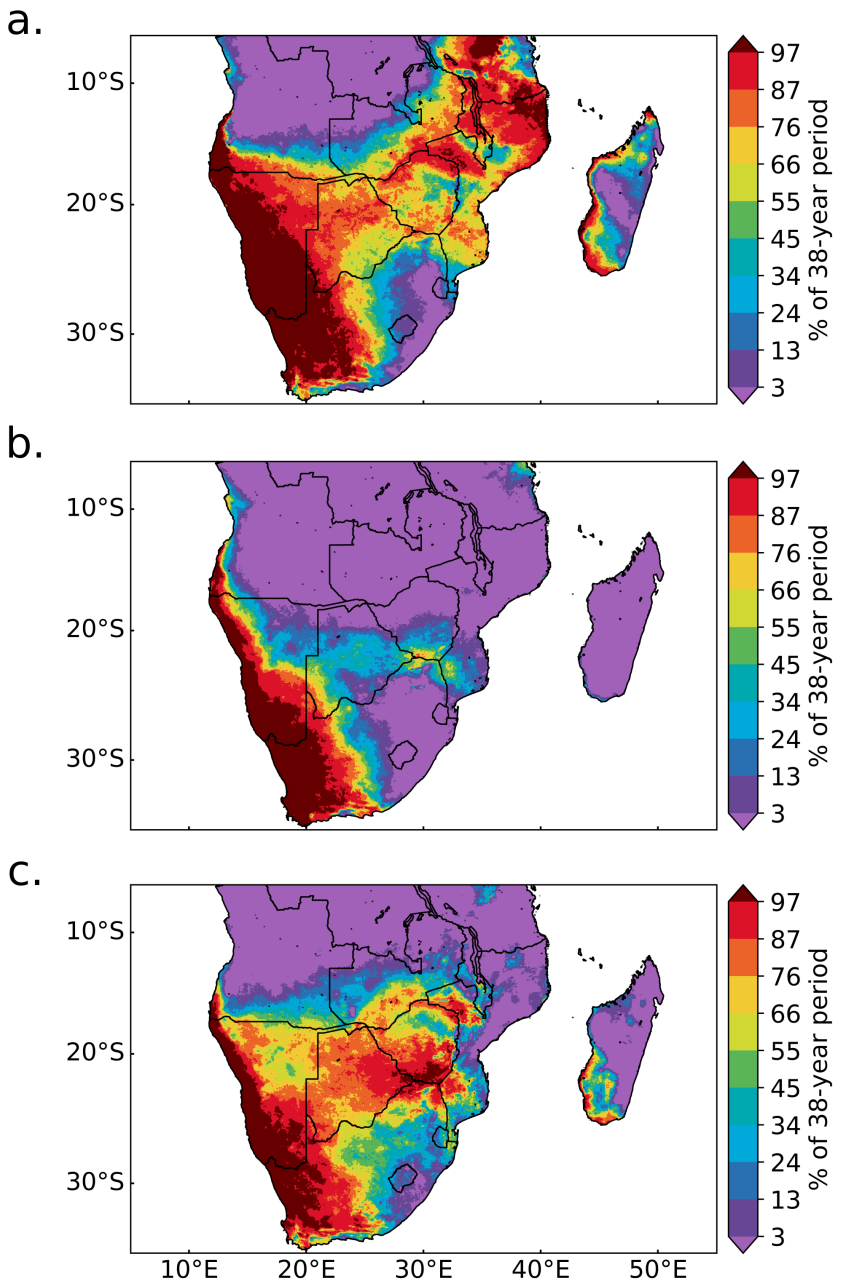

Figure 3: Intensity-frequency maps showing the percentage of the total number of seasons which consisted of at least 6 dry spells out of a maximum possible of 12 during a. ON, c. MA, and 9 out of 18 during b. DJF.

During MA, the region covering roughly 18-25°S had more than 50% of the MA seasons as dry for at least 6 pentads (half the season). In this area, a maximum was observed over the LRV where all 38 seasons had at least 6 dry spells. A relative maximum was observed over the Zambezi near the Zimbabwe-Mozambique border where more than 90% of the seasons were dry for half the season. The area covering western Lesotho and South Africa just

south of Lesotho stood out as having low frequency (0-5 seasons) compared to the surrounding regions

Dry spell frequency trends

Trends with P<0.05 were reported as significant.

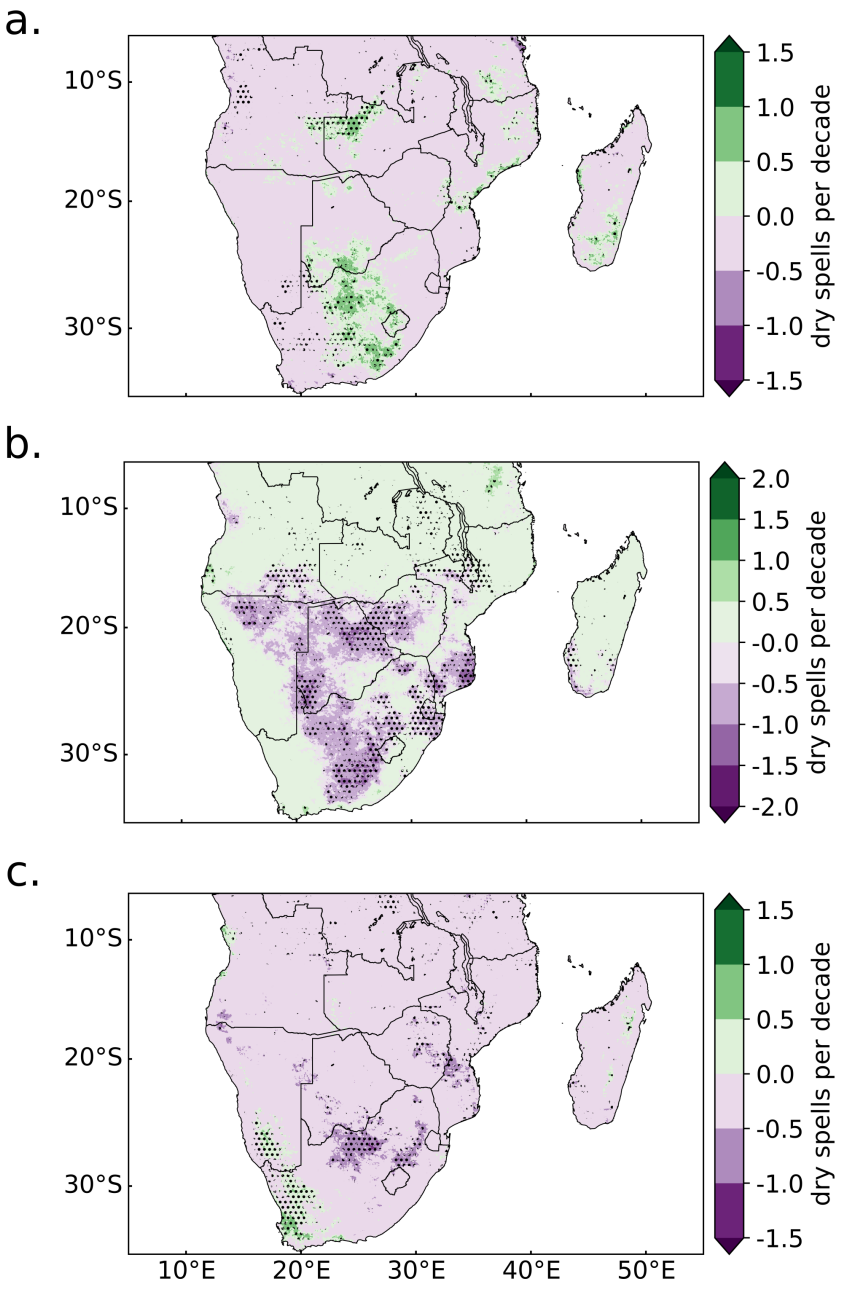

Figure 4: Trends in dry spell frequency during a. ON, b. DJF and c. MA. Contoured shading shows trends in dry spells per decade. Hatching denotes areas of significant trends (5% level) calculated over the period 1981/1982–2018/2019.

Fig. 4a shows dry spell frequency trends over southern Africa during the season of ON. Generally, trends ranged from -1 to +1 dry spells per decade, however, only a few areas showed significant trends at the 95% confidence level. Significant increasing trends were observed over northwestern Zambia extending slightly west into Angola, a stretch running from southern Botswana to central South Africa, southern Madagascar and sparse areas in Tanzania and Mozambique.

During DJF, significant trends taking place at a rate of about -1 dry spells per decade were observed in a northwest-southeast orientation across northern Namibia, southern Botswana and central South Africa, roughly along the westernmost extent of cloud bands over southern Africa and diagonal DSF gradient during austral summer (Fig. 4b). Significant decreasing trends were also found over the northern Botswana - western Zimbabwe region and over scattered areas in southern Angola, northeastern South Africa and southern Mozambique. Negative trends with magnitude of about 1 were observed over the southwestern tip of Angola and eastern Tanzania.

Trends in dry spell frequency over southern Africa during MA were negative for the most part as shown in Fig. 4c. Only few areas showed significant trends. Increasing trends of about 1 dry spell per decade were observed along the southwestern edge of Namibia and western South Africa whereas negative trends of magnitude 1 were found mostly over a few areas in South Africa. These include the North West province and sections of the Drakensberg, one stretching from northern Lesotho to Mpumalanga and the other a small area in the Limpopo Province centered at about 23°S, 30°E. Another region of decreasing trends was observed over western Zimbabwe - southern Mozambique.

4.2 Moderate wet day frequency

Mean moderate wet day frequency

Fig. 5a shows the moderate wet day frequency distribution across southern Africa during ON. With the exception of eastern DR Congo and parts of northern and central western Angola which had mean frequencies ranging from 15 to 24 wet days, southern Africa on average experienced less than a quarter of the ON season (15 days) as moderate wet days. As somewhat of an inverse of

the mean dry spell frequency distribution during ON in Fig. 2a, a minimum in moderate wet day frequency was observed over western southern Africa. This area had 0 wet days on average. Relative maximums were found to present over eastern southern Africa, near the northern Drakensberg mountain range, and central Madagascar. These areas had a mean of between 9 and 11 moderate wet days during ON.

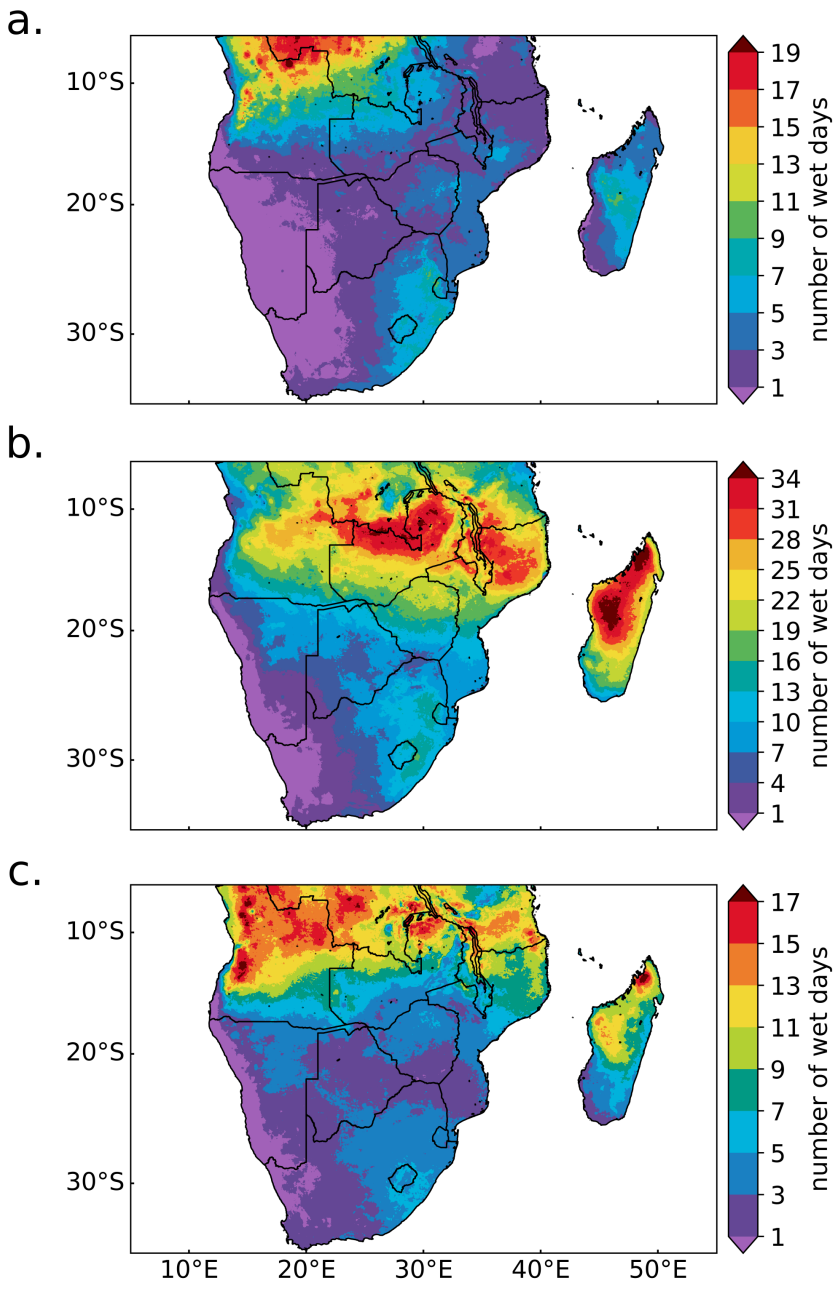

Figure 5: Moderate wet day frequency climatology over the period 1981/1982 – 2018/2019 during a. ON, b. DJF and c. MA.

Generally, the 6-19°S band on average had at least a fifth of the season (18 days) consisting of moderate wet days during DJF as shown in Fig. 5b. The highest values were found over northern Mozambique and the southern Congo basin, which covers southern DR Congo / northern Zambia. Here, mean values ranged from 28-38 moderate wet days. High frequencies of the same range were observed over northern and central Madagascar. In contrast, the southern part of the island experienced fewer than 15 moderate wet days on average. Eastern southern Africa, roughly along the Drakensberg mountain range, was also found to have relatively high mean values of between 13 and 19 wet days. Low frequencies of less than 7 days were found over the diagonal gradient in dry spell frequency observed in Fig. 2b and minimum values (0 days) along western Namibia and South Africa. The central Limpopo River Valley which had had relatively high dry spell frequencies (Fig. 2b) stood out as having relatively low frequencies of 4-7 wet days.

Most of southern Africa had a mean moderate wet day frequency of below 10 days during MA as shown in Fig. 5c . Minimum values were observed over the western coast of southern Angola, Namibia and South Africa where the season on average experienced no moderate wet day. Mean frequencies of 10 or more days were found over Angola, southern DR Congo, northern Zambia, western and southern Tanzania, and central and northern Madagascar. Maximum values of 17-20 wet days were observed over areas scattered across western Angola and at the northern tip of Madagascar.

Intensity-frequency maps

Intensity-frequency maps in Fig. 6 show the susceptibility of an area to experiencing moderate wet days. Values plotted in Fig. 6a show the percentage of the total number of ON seasons having at least 10 moderate wet days. During the 38 year period, most of southern Africa had no season consisting of 10 or more wet days. Maximum values were observed over parts of central DR Congo, where 100% of the seasons (38) had at least 10 days that were experienced as wet. This number decreases in the surrounding regions of northern Angola and central DR Congo to 76-97% (28-37 seasons). Relative maximums were observed over eastern South Africa and central Madagascar, where 24 -45% of the seasons (9-17) had 10 or more moderate wet days.

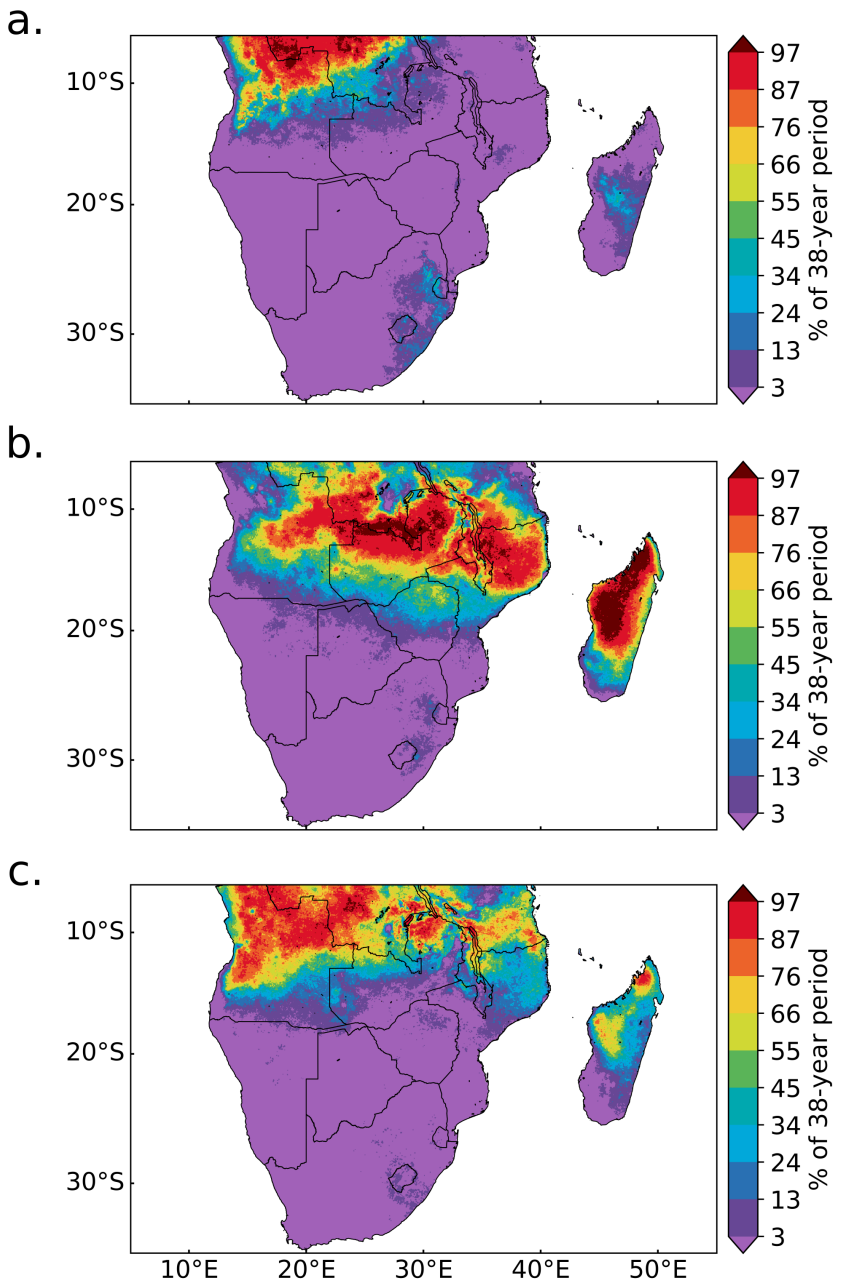

Figure 6: Intensity-frequency maps showing the percentage of the total number of seasons which consisted of at least 10 moderate wet days out of a maximum possible of 60 during a. ON, c. MA and, 20 out of 90 during b. DJF.

Percentages in Fig. 6b show the proportion of summer seasons with at least 20 moderate wet days. Less than 50% of the summers consisted of 20 or more moderate wet days over subtropical southern Africa. This number increased to 75-100% over the tropical region stretching from central Angola to northern Mozambique. Maximum percentages were observed over northern and central Madagascar, near the Zambia / DR Congo border and northern Mozambique

where all 38 summers had 20 or more wet days. Two relative maximums were observed over eastern South Africa near the northern and southern sections of the Drakensberg. The percentage of seasons having at least 20 moderate wet days ranged between 24 and 34 (9-13 seasons) over these areas.

Values in Fig. 6c show the percentage of MA seasons that had 10 or more moderate wet days. Southwestern Madagascar and the area south of about 17°S over the southern African mainland generally had fewer than 5 seasons with at least 10 wet days. This number increased over northern and central Angola, southern and central DR Congo, northern Zambia and southern Tanzania, areas that had between 25 and 37 seasons (66-100%) experiencing 10 or more wet days. Percentages of the same range were also observed over central and northern Madagascar. A maximum was observed centred around 8°S, 24°E where all 38 seasons had at least 10 moderate days.

Moderate wet day frequency trends

Most of southern Africa had increasing wet day trends during the ON season however only a few areas showed significant trends at the 5% level (Fig. 7a). Significant increasing trends ranging from about 1-2 moderate wet days were observed over two discrete areas in northern Angola/ eastern DR Congo, along 16°and 21°E. Decreasing significant trends of a magnitude of about 1 were found over northern Angola, southern DR Congo and South Africa, cutting across the North West and Free State provinces. West of this region in central South Africa is a region of weak significant increasing trends of about 1 wet day per two decades.

As with ON, most of southern Africa showed increasing trends in moderate wet day frequency during DJF as shown by Fig. 7b. Significant increasing trends of 1-4 wet days per decade were observed over central Angola near the Angolan plateau, the DR Congo - Zambia border, eastern Botswana / western Zambia and the northern tip of Madagascar. This range decreases to 1-2 over the strip running from the Drakensberg's most southern extent in the Eastern Cape northwards to about 27°S, 29°E. There was a small area of significant decreasing trends of about 1-2 wet days per decade over southern DR Congo.

During MA, most of southern Africa showed an increase in moderate wet day frequency, however only a few areas had significant trends (Fig. 7c). Positive trends ranging between 1 and 2 wet days per decade were observed near

the Angola - DR Congo border centred along 22°E, the DR Congo - Zambia border and over northern Botswana. Weaker increasing trends of about 1 wet day per two decades were found over the west coast of southern Namibia and South Africa. A few areas over northern Angola, northern Mozambique and the west coast of Madagascar showed a decreasing trend of about -1 wet day per decade.

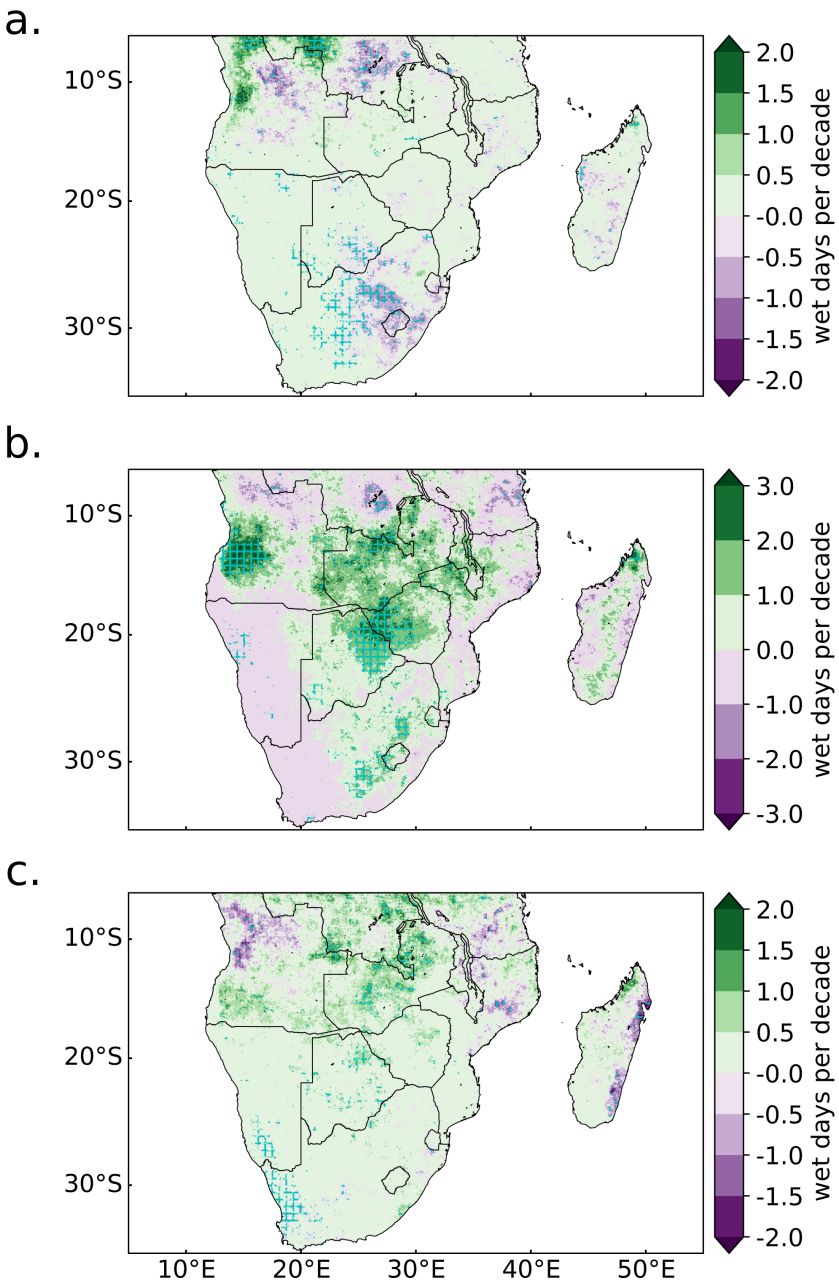

Figure 7: Trends in moderate wet day frequency during a. ON, b. DJF and c. MA. Contoured shading shows trends in wet days per decade. Hatching denotes areas of significant trends (5% level) calculated over the period 1981/1982 – 2018/2019.

4.3 Potential mechanisms

Indices of climate modes known to influence rainfall over southern Africa namely, ENSO, SIOD and SAM were correlated with and DSF and MWDF over southern Africa during ON, DJF and MA. DSF and MWDF were also correlated with an index of tropical SE Atlantic SST events. Possible mechanisms driving changes in dry spell and wet day frequencies across southern Africa were examined through regressions with atmospheric and SST fields over two areas in southern Africa during DJF. Region 1 is found in South Africa, southwest of Lesotho. This region was chosen since it forms part of the DSF diagonal gradient and showed significant trends in DSF and MWDF during DJF. Additionally, it is located within an important South African agricultural area where sheep keeping predominates. Region 2 extends slightly eastwards from western Botswana to South Africa and Zimbabwe. It was selected as it is representative of the meridional gradient in DSF and forms part of the drought corridor. During DJF, a relative DSF (MWDF) maximum (minimum) and significant trends in DSF were found in this area. Forming part of the Limpopo River Basin (LRB), this region supports both subsistence and commercial agriculture. It is also home to the Mapungubwe National Park. Results of computed correlations and regressions will be outlined in this subsection and the interpretation given in the Discussion section.

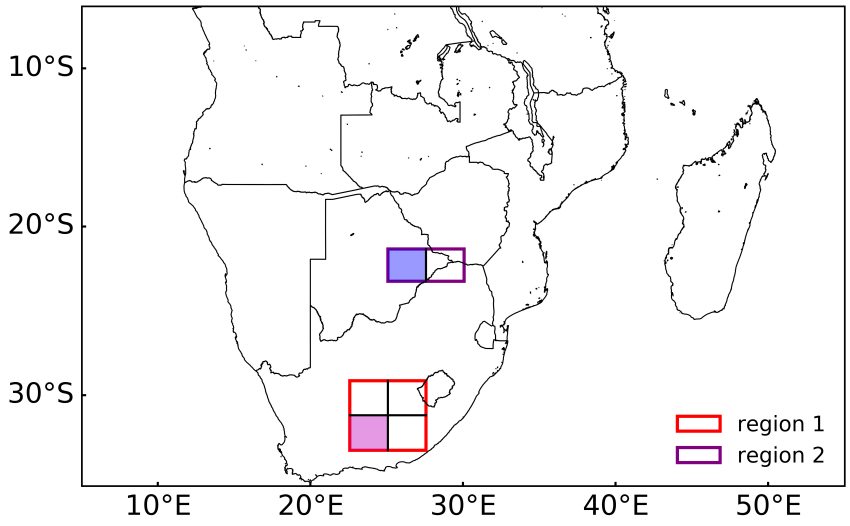

Figure 8: Map showing region 1 and 2. Subregions within these polygons are those over which DSF and MWDF were regressed against atmospheric and SST fields. Shaded polygons show subregions whose maps are displayed and whose results are representative of other subregions within each region.

Correlations with climate modes

Figures displaying correlations with ENSO and with SST over the SE Atlantic will be shown for all three seasons. However, for SIOD and SAM, only those displaying correlations during DJF will be shown as relationships were most robust over spatially coherent areas during this season. Figs. A2 and A3 in the Appendix A1 section show correlations with SIOD and SAM indices, respectively, during ON, DJF and MA. Correlations with P $<$0.05 at the 95 % confidence level are reported as significant.

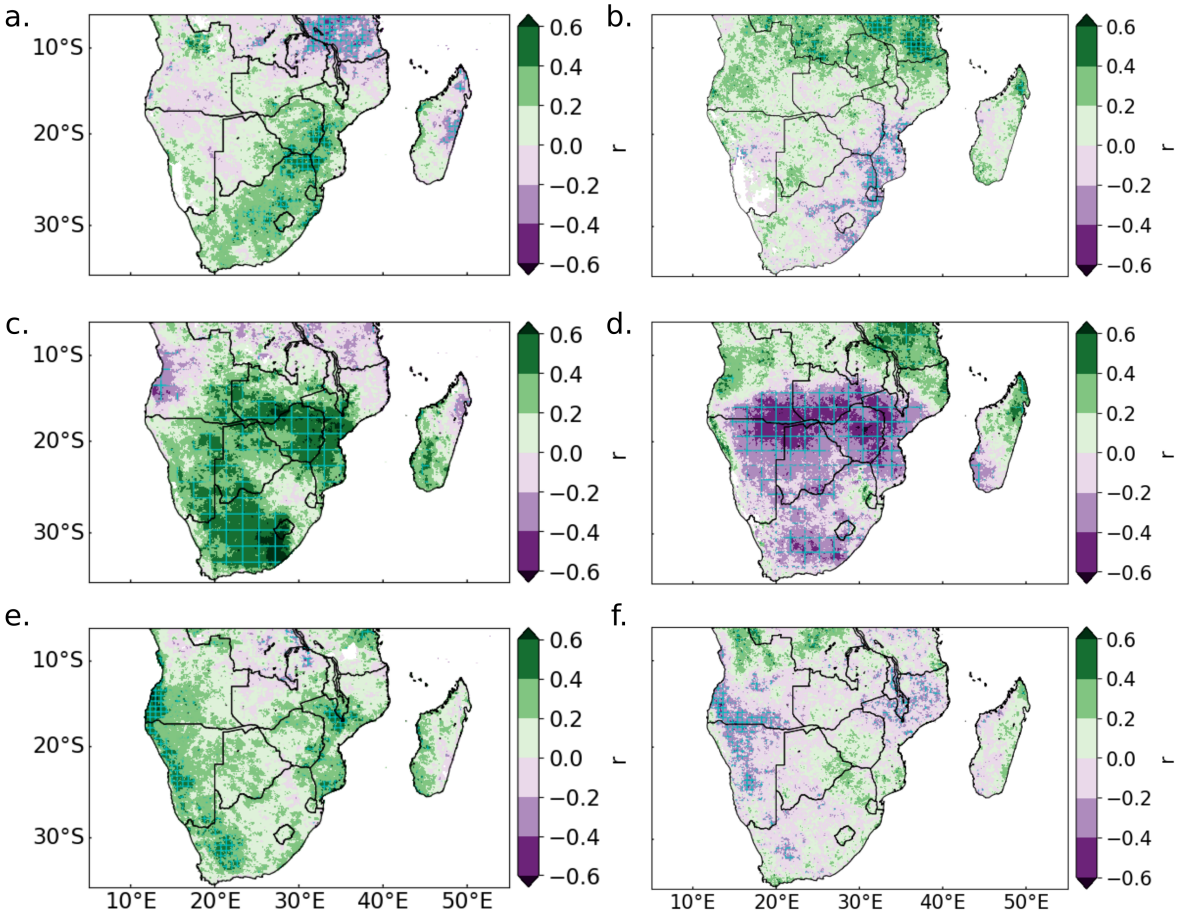

Figure 9: Correlation coefficients between the Niño 3.4 index and dry spell frequencies during a. ON, c. DJF and e. MA, and with moderate wet day frequencies during b. ON , d. DJF and f. MA. Hatching denotes areas of significant correlations (95% confidence level) calculated over the period 1981/1982 – 2018/2019

During ON, ENSO was found to have a positive significant relationship with DSF over parts of southeastern Africa, as shown by Fig. 9a. These include northern Angola, southern Zimbabwe - northern South Africa, the Zimbabwe -

Mozambique border near the Chimanimani Mountains and a few scattered regions over central and eastern South Africa, where r values ranged from 0.32 to 0.62. By contrast, DSF over Tanzania and parts of western Madagascar were negatively correlated with ENSO (-0.32 to -.62). For MWDF, a positive significant relationship was observed over Tanzania and northern Madagascar (0.32-0.74) whereas southern Mozambique and the north eastern coast of South Africa showed significant negative correlations ranging from -0.32 to -0.64 (Fig. 9b). ENSO was shown to be significantly correlated with DSF and MWDF over much larger areas during DJF. Fig. 9c shows that with the exception of northeastern Madagascar, western Angola and sparse areas in southern DR Congo and Tanzania, DSF over of southern Africa had a positive relationship with ENSO with significant r values ranging from 0.32 to 0.78. Conversely, MWDF roughly south of 15°S was significantly negatively correlated with ENSO (-0.32 to -0.77). Exceptions include the northern half of the Namibian Coast and northeastern South Africa near Eswatini. Over Madagascar, an inverse relationship between ENSO and MWDF was observed over the southwestern part of the island and over the north, a positive relationship (Fig. 9d). During MA, significant correlations covered more sparse areas of southern Africa. According to Fig. 9e, DSF over southern Africa had a positive relationship with ENSO over the western coast of Angola, Namibia, western South Africa and parts of Mozambique (0.32-0.71). For MWDF, significant negative correlations ranging from -0.32 to -0.63 with were found to be present over southern Angola, Namibia and parts of Malawi (Fig. 9f).

SIOD and SAM were significantly correlated with DSF / MWDF mostly during DJF. During ON, weak non-significant positive correlations between SIOD and DSF were present over southern Africa (Fig A2a) whereas correlations with MWDF showed a mix of non-significant positive and negative correlations as shown in Fig A2b. SIOD was significantly correlated with DSF / MWDF mostly over southeastern Africa during DJF. The area of significant correlations with DSF covered western Botswana, Zimbabwe and southern Mozambique with values ranging from -0.32 to -0.67 as shown in Fig. 10a. A few areas of significant positive correlations were observed over the coasts of southern Angola, northern Namibia, northern Mozambique and eastern Madagascar. SIOD had a positive relationship with MWDF over much of southern Africa during austral summer. Significant correlations were found to be present over Botswana, Zimbabwe, Zambia, southern Mozambique and southern Madagascar where values ranged from 0.32 to 0.75 (Fig. 10b). During MA, SIOD has a significant negative relationship with DSF over the region stretching from southern Angola

to southern Mozambique (Fig. A2e) and a non-significant positive relationship with MWDF over southern Africa (Fig. A2f).

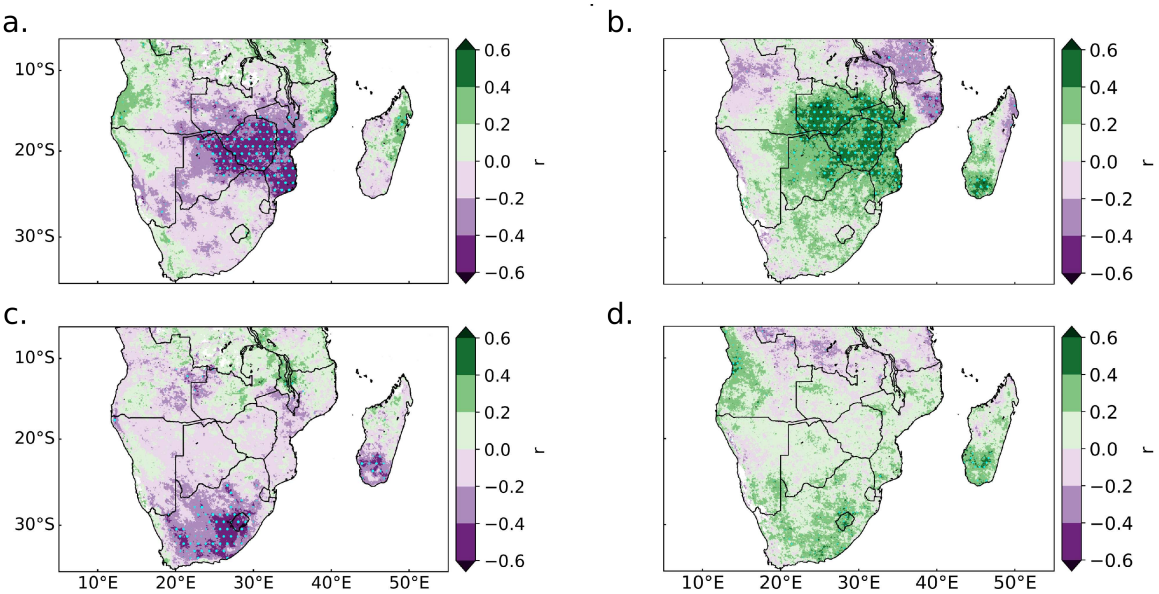

Figure 10: Correlations between a. the SIOD index and dry spell frequencies, b. the SIOD index and moderate wet day frequencies, c. the SAM index and dry spell frequencies and d. the SAM index and moderate wet day frequencies. Hatching denotes areas of significant correlations (5% level) calculated over the period 1981/1982 – 2018/2019 during DJF.

As shown in Figs. A3a and b, during ON, DSF and MWDF correlations with SAM were non-significant over southern Africa. SAM however had a significant relationship with DSF and MWDF during DJF. Significant correlations with DSF were found over Lesotho and the area covering western and central South Africa as shown in 10c. Only a few areas showed significant correlations with MWDF with values ranging from 0.37 to 0.45. These include western Angola, Lesotho, southern Madagascar and sparse areas in South Africa as shown in Fig. 10d. During MA, non-significant correlations were observed over southern Africa (Figs. A3e and f).

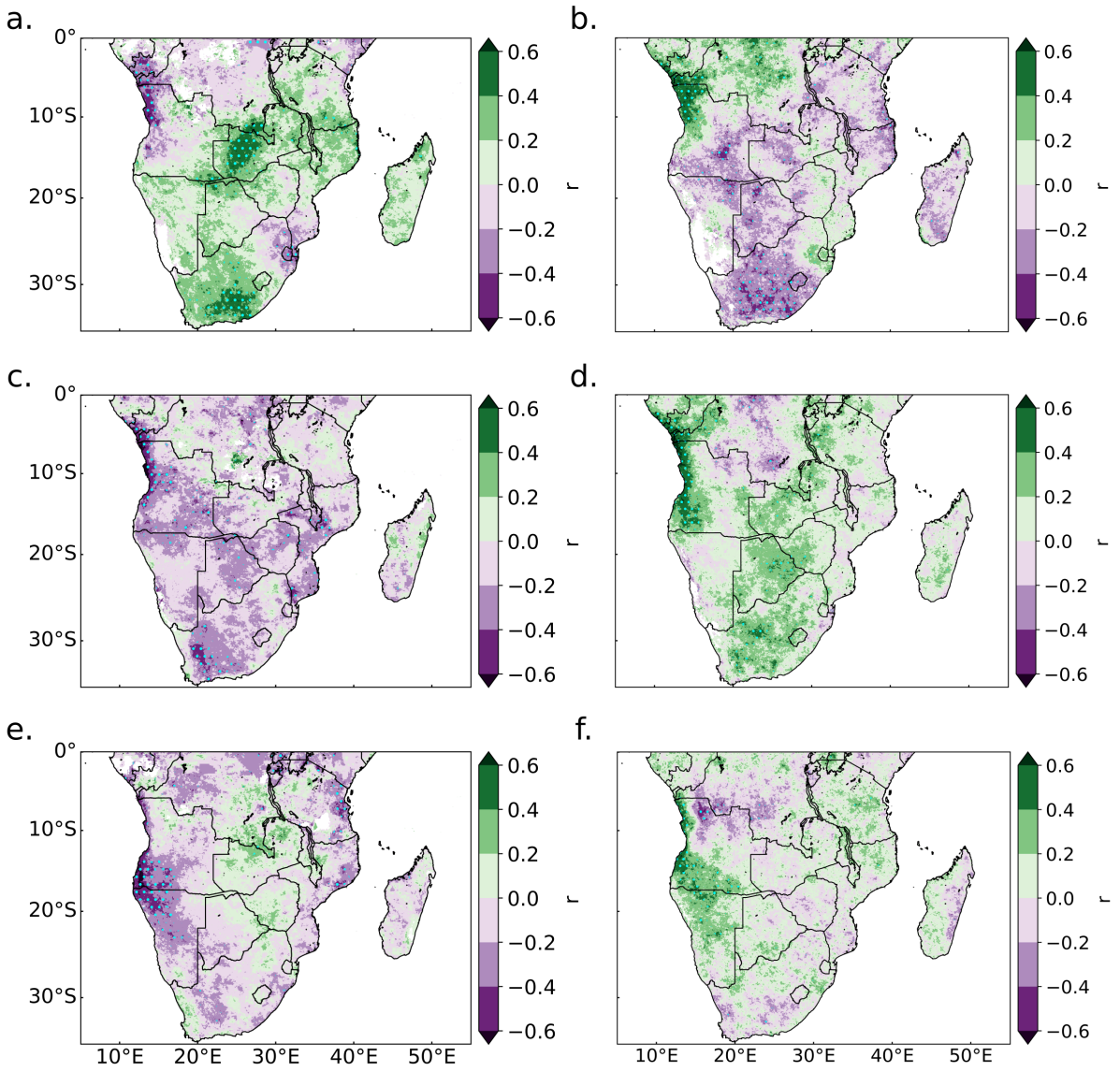

Figure 11: Correlation coefficients between an index of SST averaged over the tropical SE Atlantic (10-20°S, 8°E to coast) and dry spell frequencies during a. ON, c. DJF and e. MA, and with moderate wet day frequencies during b. ON , d. DJF and f. MA. Hatching denotes areas of significant correlations (95% confidence level) calculated over the period 1981/1982 – 2018/2019

Correlations between an index of warm events in the tropical SE Atlantic and DSF/ MWDF over southern Africa during ON, DJF and MA are shown in Fig. 11. During ON, SST over the SE Atlantic was found to be negatively correlated with DSF over the coasts of Congo, DR Congo, northern Angola and over Eswatini. Significant r values over these areas ranged from -0.32 to -0.72. The two regions showing significant positive correlations during ON included one running from southern DR Congo through western Zambia and the

other southern South Africa (r=0.4-0.6). Correlations with MWDF over southern Africa showed the opposite signal of those with DSF for the most part. There was an area of positive correlations over the region covering the coasts of Congo, DR Congo and northern Angola (r=0.32-0.76). In contrast, negative correlations were observed over southeastern Angola, parts of northern Namibia and Botswana and the regions of western and central South Africa. Over these areas correlations ranged from -0.32 to -0.68.

During DJF, correlations with DSF were mostly negative over southern Africa. Significant correlations ranging from -0.32 to -0.77 were observed over the coasts of Congo, DR Congo and Angola, southwestern South Africa, southeastern Angola and scattered areas in Botswana, Zimbabwe and Mozambique. The relationship between MWDF over southern Africa and SST in the tropical SE Atlantic was mostly positive with significant correlations observed along the coasts of southern Gabon, Congo, DR Congo and Angola (r=0.33-0.6). Weaker positive correlations were also observed over western Botswana and parts of western and central South Africa. A few regions of negative correlations were found scattered over the interior of DR Congo.

Significant correlations were observed over a smaller area during MA. For DSF, negative correlations were observed over southwestern Angola and northwestern Namibia with r values ranging from -0.32 to -0.75. Smaller areas over the coast of Tanzania and northern Mozambique also showed significant negative correlations, though weaker. Significant positive correlations with MWDF were observed along the coast of Angola and over the region covering southern Angola and northern Namibia (0.32-0.69). There was a small region of negative correlations over northern Angola - southern DR Congo where r values ranged from -0.32 to -0.69.

Region 1

Only regressions with DSF are shown as those with MWDF showed the approximately the opposite. In Fig. 12, DSF (MWDF) regressions with geopotential height at 500 hPa showed a positive (negative) sign roughly over Antarctica and negative (positive) over the location of the southern hemisphere westerlies, a pattern reminiscent of SAM. Additionally, DSF (MWDF) had a positive (negative) relationship with Z500 over the Botswana High region. These relationships and others will be further detailed in the Discussion section. Fig. 13a

plots DSF (MWDF) over region 1 regressed against omega at 500 hPa and indicates that a positive (negative) relationship with omega existed over much of subtropical southern Africa, extending diagonally from Angola to the east coast of South Africa and Mozambique. Likewise, DSF (MWDF) over region 1 had a positive (negative) relationship with OLR over the interior of subtropical southern Africa (Fig. 13b). Reminiscent of ENSO SST anomalies, SST over the central and eastern tropical Pacific was observed to have a fairly strong positive (negative) relationship with DSF (MWDF) over region 1 as shown in Fig. 14b . Additionally, DSF (MWDF) had a significant negative (positive) relationship with SST in the tropical SE Atlantic. Moisture flux over the South Atlantic was positively (negatively) associated with DSF (MWDF) whereas that over the southern Indian Ocean had a negative (positive) relationship with DSF (MWDF) (Fig. 14a).

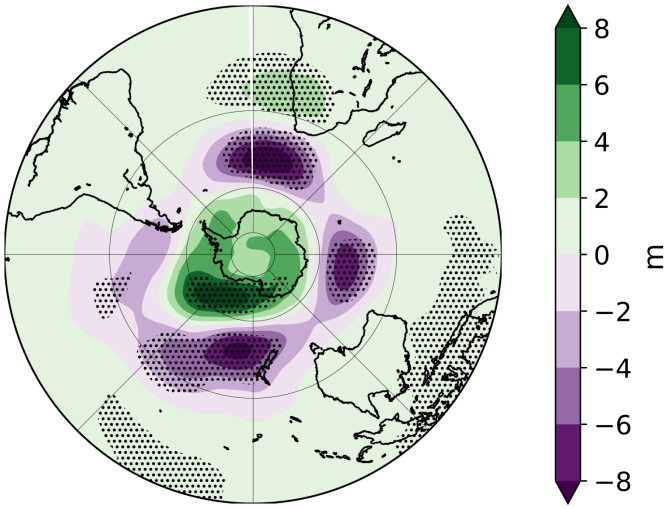

Figure 12: Regressed geopotential height at 500 hPa (shaded contours in m) with respect to area averaged dry spell frequency over region 1 over the period 1981/82-2018/19 during DJF. Stippling denotes significant regressions ($p < 0.05$).

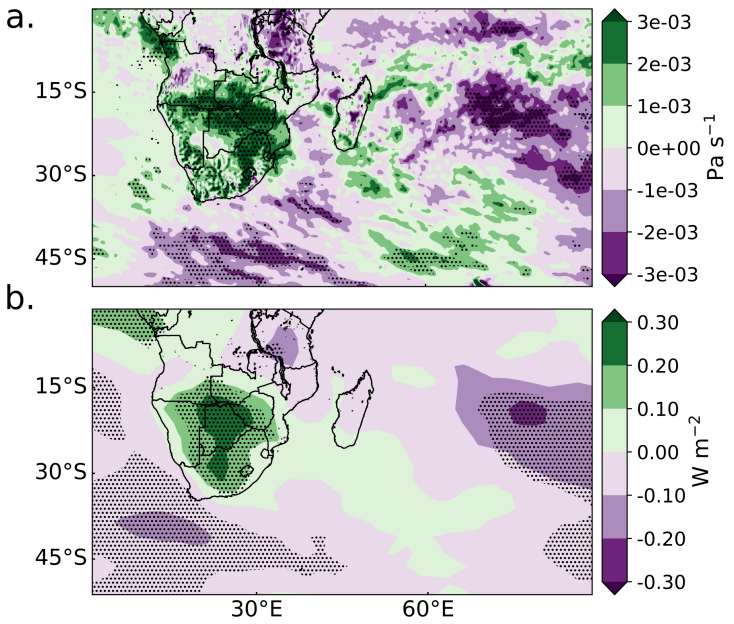

Figure 13: Regressed a. omega at 500 hPa (shaded contours in Pa s^{-1}) and b. OLR (shaded contours in W m^{-2}). Regression is calculated with respect to area averaged dry spell frequency over region 1 over the period 1981/82-2018/19 during DJF. Stippling denotes significant regressions ($p < 0.05$).

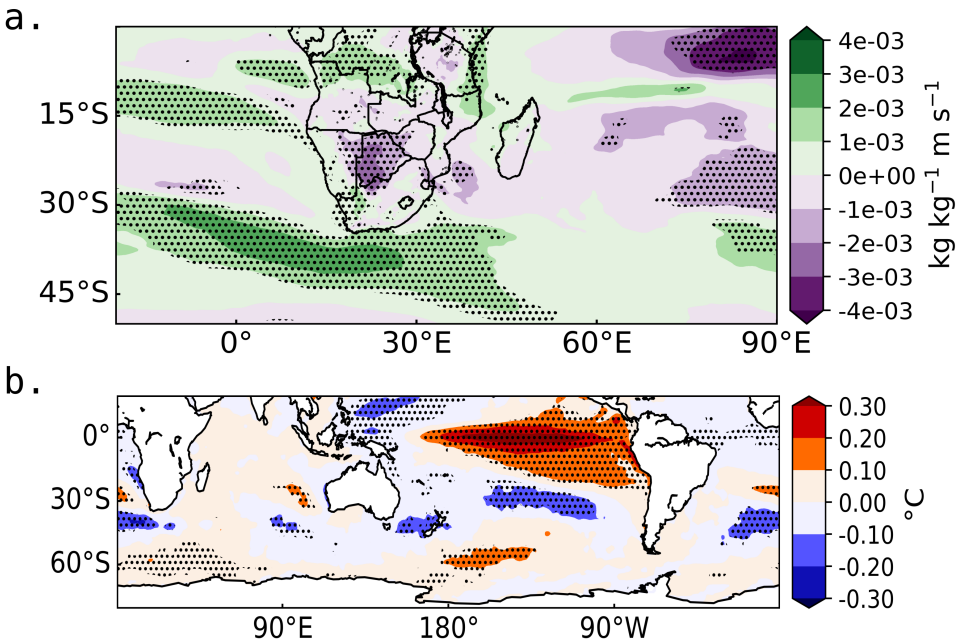

Figure 14: Regressed a. moisture flux at 850 hPa (shaded contours in kg kg^{-1} m s^{-1}) and b. SST (shaded contours in °C). Regression is calculated with respect to area averaged dry spell frequency over region 1 over the period 1981/82 - 2018/19 during DJF. Stippling denotes significant regressions ($p < 0.05$).

Region 2

Fig. 15 shows that there was a negative (positive) relationship between DSF (MWDF) and 500 hPa geopotential height over two areas of the subtropical southern Indian Ocean, one near the southern Mozambique Channel and the other centered along 90°E, in the Mascarene High region. As with region 1 DSF (MWDF) over region 2 had positive (negative) regressions with omega over the southern Africa interior, however in this case the area extended southeastwards to the southwest Indian Ocean (Fig. 16a). Similarly, DSF (MWDF) had a positive (negative) relationship with OLR over this region as shown in Fig. 16b. In Fig. 17b, regressions with SST show that DSF (MWDF) had a negative (positive) relationship with SST in the southwest Indian Ocean and positive (negative) with those off Australia in the eastern Indian Ocean, a pattern reminiscent of the SIOD. Additionally, DSF (MWDF) had a significant negative (positive) relationship with SST over the eastern and western Pacific Ocean. DSF (MWDF) over region 2 is negatively (positively) associated with easterly moisture fluxes from the southern Indian Ocean (Fig. 17a).

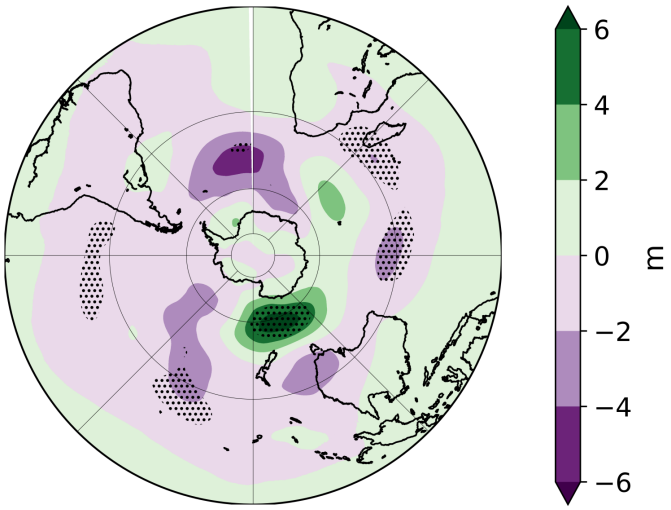

Figure 15: Regressed geopotential height at 500 hPa (shaded contours in m) with respect to area averaged dry spell frequency over region 2 over the period 1981/82-2018/19 during DJF. Stippling denotes significant regressions ($p < 0.05$).

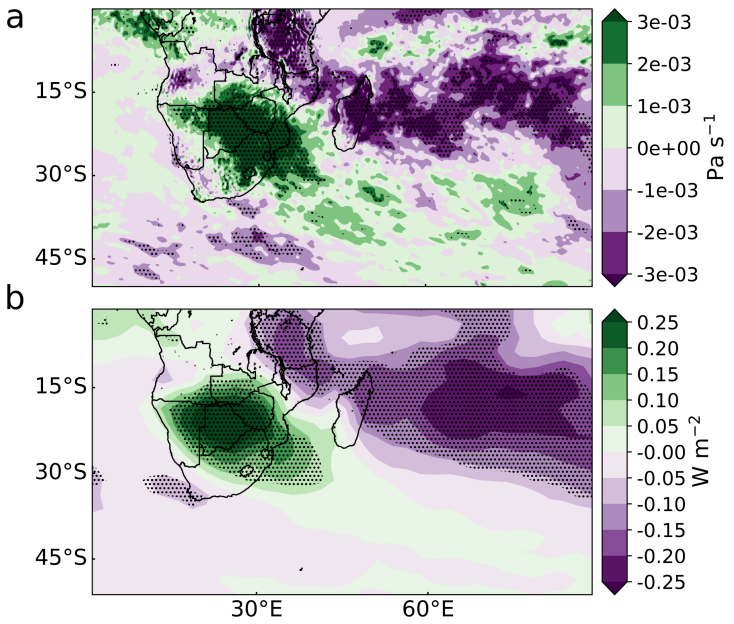

Figure 16: Regressed a. omega at 500 hPa (shaded contours in Pa s^{-1}) and b. OLR (shaded contours in W m^{-2}). Regression is calculated with respect to area averaged dry spell frequency over region 2 over the period 1981/82-2018/19 during DJF. Stippling denotes significant regressions (p $<$0.05).

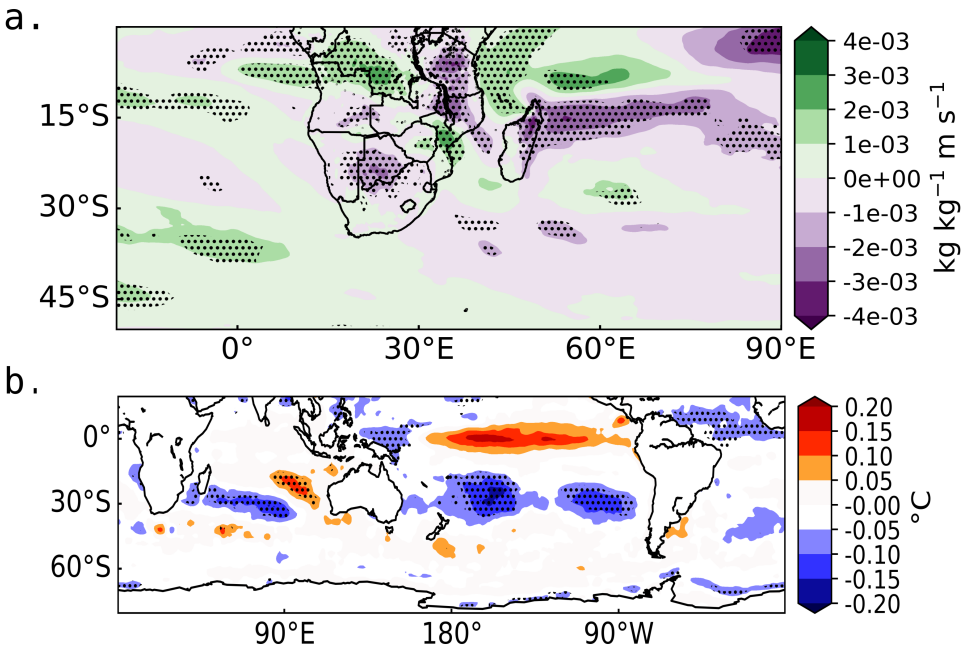

Figure 17: Regressed a. moisture flux at 850 hPa (shaded contours in kg kg^{-1} m s^{-1}) and b. SST (shaded contours in °C). Regression is calculated with respect to area averaged dry spell frequency over region 2 over the period 1981/82-2018/19 during DJF. Stippling denotes significant regressions (p $<$0.05).

5 Discussion

The mean distribution of DSF and MWDF over tropical southern Africa from ON to MA is consistent with that of seasonal totals as areas of low seasonal rainfall generally correspond to areas of high (low) DSF (MWDF) and vice versa (section 6). It follows the north-south displacement and change in latitudinal extent of the African tropical rain belt which begins its southward movement into southern Africa in October, the onset of the rainy season in southern Africa (Reason, 2017). The rain belt moves farther south during DJF when it is present over a greater latitudinal extent across the region. During MA it retreats slightly northward and decreases in latitudinal extent (Nicholson, 2018). The shifts in the position and breadth of the rain belt roughly correspond to the expansion of the region of low DSF \high MWDF region which occupies northern Angola and DR Congo during ON and roughly the 6-18 °S band during DJF. Thereafter, during MA, this region is restricted to northern Angola, DR Congo and Tanzania. Near the southern boundary of the tropical rain belt is the meridional gradient in DSF, which is most prominent during DJF. While the gradient varies in position and strength through the seasons, DSF generally increases southwards as one crosses the southern boundary of the tropical rain belt. The meridional gradient exists in part due to changes in regional topography and the presence of the MCT which discourages direct easterly moisture transport over subtropical southeastern Africa (Barimalala et al., 2018, 2020). The diagonal gradient in DSF is present over western southern Africa from southwestern Angola to western South Africa through all three seasons however it it strongest during DJF, when its location lines up with the western boundary of the typical area where continental cloud bands occur. The NW-SE orientation of TTTs which contribute significantly to summer rainfall (Todd and Washington, 1999) contributes to the orientation of this gradient. Further, the span of the rain belt over tropical southern Africa is smaller to the west (Nicholson, 2018).

The influence of topography on rainfall is expected to be observable on the windward slopes and peaks of mountains (relatively low DSF / high MWDF) and over areas which fall within the rain shadow (relatively high DSF / low MWDF). Low DSF over eastern Madagascar is due to enhanced rainfall occurring on the windward side of the mountain range running lengthwise across country. According to Jury et al. (1995), the east coast of the island experiences significantly higher rainfall than the west due to being on the wind-

ward side of the mountain. High MWDF is prominent especially over northern and central Madagascar where the highest mountain peaks are located (Randriamahefasoa and Reason, 2017). Southwestern Madagascar lies in the rainshadow and thus has relatively high DSF and low MWDF (Jury et al., 1995; Randriamahefasoa and Reason, 2017). Over the southern African mainland, relatively low DSF and high MWDF found over eastern South Africa are a result of orographic forcing on the eastern windward slopes of the Drakensberg. Other topographic effects are observed east of Mulanje Massif (on the windward side) during ON, where there is relatively low DSF and high MWDF. Additionallly, through all the seasons, low DSF is found over the central Zimbabwe / Mozambique border roughly over the highest peaks of the Chimanimani mountain range (Wursten et al., 2017). During ON and DJF, on the east coast of South Africa, around the Kwa Zulu Natal / Eastern Cape region, low DSF may be associated with ridging anticyclones which interact with westerly frontal systems to produce onshore flow and heavy rainfall over this coastal region located near the Drakensberg escarpment (Weldon and Reason, 2014; Ndarana et al., 2018; Mahlalela et al., 2020).

Another interesting feature of DSF climatology is the relative maximum in the central LRV observed during DJF and MA. This maximum is consistent with the relative minimum in seasonal rainfall found over the LRV during DJF and MA (Fig. A1) and exists in part due to the topography of the low-lying Limpopo River Valley which is unfavourable for the development of convective systems (Rapolaki et al., 2019). Additionally, the MCT which develops due to the dynamical adjustment of the easterlies over the high topography of Madagascar, discourages the direct easterly moisture flux transport from the southern Indian Ocean to the LRV (Barimalala et al., 2018, 2020).

Intensity-frequency maps in Fig. 3 indicate the susceptibility of an area to experiencing meteorological drought since they show the number of seasons having half of the season containing dry spells. Usman and Reason (2004) identified a preferred region of high DSF located across 20 to 25°S during DJF, where more than half of the season was often made up of dry spells. This zone was termed the drought corridor and can be observed in Fig 3b lying roughly across a more tightly defined band, 22-24°S. Here summers frequently had half of the season made up of dry spells. Over the same region is an area of relatively high coefficients of seasonal rainfall variation (section 6) which shows that considerable interannual rainfall variability is experienced within the drought corridor. This study reveals a core in the drought corridor located

in the central LRV which is absent in Usman and Reason (2004) due to the lower resolution of the data used (2.5°). The core is the region where 85-100% of the summers had 9 or more dry spells and is thus highly susceptible to multi-year droughts despite being located relatively near moisture sources of the tropical west and southwest Indian Ocean (Rapolaki et al., 2020). The drought corridor covers 18-25°S during MA and corresponds to a region of low seasonal rainfall and relatively high coefficients of variation (CVs) (Fig. A1). Covering a larger area than during DJF, the core of the drought corridor during MA is found in the northern Limpopo River Basin, where 100% of seasons had half of the season made up of dry spells.

Intensity frequency maps in Fig. 6 show the susceptibility of an area to the occurrence of moderate wet days. During DJF, the area where at least 50% of the seasons were made up of 20 or more wet days stretches from northern Mozambique to central Angola and corresponds to the region of relatively high seasonal rainfall ($>$700 mm) over the tropical southern Africa (Fig. A1). During ON and MA, this region is restricted to wet areas of tropical convergence north of 15°S (10 or more wet days). Topographic incluences are observed over the mountain peaks of northern and central Madagascar and eastern South Africa to a lesser extent. Intensity-frequency maps can be understood to show the number of summers with 2 wet days every nine days during DJF and 1 every 6 days during ON and MA. If wet days are evenly distributed within the season and other physical factors are satisfied, then an area may be well suited to rain-fed agriculture. Most of southern Africa however had less than a third of the seasons analysed having 10 (ON, MA) and 20 or more wet days (DJF), suggesting that rainfall in subtropical southern Africa is unreliable for agricultural needs.

During ON, significant increasing trends occurring at a rate of about 1 dry spell per decade over southern Botswana and central South Africa, the southern extent of the diagonal DSF gradient present during ON, imply that a strengthening of the gradient has occurred over the region in the recent years. A shift towards increased DSF during ON is consistent with projected early summer drying over southern Africa. In Dunning et al. (2018), large areas in southern Africa were projected to have later onset dates during the summer rainy season. Munday and Washington (2019) showed that there is a broad consensus among climate models of a projected decline in rainfall during OND, the season of rainfall onset. While this study does not analyse trends in onset and withdrawal dates, the increase in DSF during ON may point to a shift in

the onset date (later onset) and shortening of the rainy season over this area which could affect the germination and growth phase of crops over the western fringes of the maize growing region of South Africa. In contrast to ON trends, decreasing trends of the same magnitude occurring over northern Namibia, southwest Botswana and central South Africa, the approximate location of the diagonal DSF gradient present during DJF, suggest a weakening and westward shift of the gradient during the summer season. Decreasing DSF trends in western Botswana - eastern Zimbabwe suggest a shift towards more consistent rainfall and a narrowing of the DJF drought corridor. If these trends in DSF persist, they may have significant implications for agricultural land use. Over South Africa, for example, significant trends occur on the margins of the maize growing region which is located in the wetter eastern part of the country (Mangani et al., 2019). Cattle keeping and sheep farming are more common farther west in the arid areas (Cloete and Olivier, 2010).

Increasing trends in MWDF (1 wet day per two decades) and DSF (1 dry spell per decade) over central South Africa during ON are seemingly in opposition to each other. Moderate wet day trends are much weaker thus trends over this region may signal the occurrence of heavier rainfall but increase in drought. Consistent with this change is the decrease in light wet days (2-9 mm) occurring roughly over the same region during ON (Fig. A4). Northeast of this region and north of Lesotho is an area of decreasing MWDF (1 wet day per decade) coupled with an increase in DSF which indicates drying of the region. During DJF, increasing trends observed in Fig. 7c occur over important agricultural areas in southern Africa. Maize growing predominates in central Angola and the South African region stretching northwest from the central Drakensberg towards Johannesburg whereas grazing is more common in the area extending southwest from from southern Lesotho. The increase in the occurrence MWD over these regions may be favourable for agriculture especially over the latter region, which, if trends persist, may open up to more mixed farming. Other areas of statistically significant increasing trends near the DR Congo-Zambia border and over the western Botswana-Zimbabwe region are more sparsely settled. It is noteworthy that a significant increase of about 3 wet days per decade over the MWDF maximum near the southern DR Congo-Zambia border which on average has 34 to 36 moderate wet days.

The relationships between climate modes and DSF / MWDF over southern Africa are consistent with what has been published about relationships with seasonal rainfall. The dipole pattern in correlations with ENSO during ON,

when DSF (MWDF) over Tanzania had a significant negative (postive) relationship with ENSO compared to southeastern Africa where correlations were positive (negative), is consistent with the opposing influences of ENSO on East (positive relationship) and southern African (negative relationship) rainfall (Nicholson, 2000). During DJF, ENSO had the most widespread significant correlations over the region since it is the dominant driver of interannual variabilty of southern African rainfall (Nicholson and Entekhabi, 1987; Nicholson and Kim, 1997; Reason, 2001) and events are phase-locked to austral summer (Ham et al., 2013; Chen and Jin, 2020). It is worth mentioning that the spatial correlation pattern with DSF is similar to that with seasonal total rainfall during DJF (Fig. A5). However, significant correlations with DSF occur over a smaller region and exclude a few areas such as Tanzania, where significant correlations with seasonal totals occurred. During MA, significant correlations were present over much smaller areas as this is typically the decaying phase of ENSO, when ENSO-related SST anomalies decrease in amplitude (Lee et al., 2014).

Like ENSO, SIOD events are seasonally locked to austral summer (Behera and Yamagata, 2001). The relationship with DSF and MWDF is consistent the SIOD's influence on southern African rainfall. Positive (negative) SIOD phases tend to be associated with above (below) rainfall over parts of southeastern Africa (Behera and Yamagata, 2001; Reason, 2001). Circulation anomalies associated with positive SAM phases are known to be favourable for above average rainfall over parts of southern Africa during summer (Gillett et al., 2006; Malherbe et al., 2014). This is consistent with SAM's negative relationship with DSF over South Africa and southern Madagascar during DJF as lower DSF is associated with positive SAM phase.

Warm SST anomalies over the tropical SE Atlantic occurring during late summer (February-April) have been shown to be associated with increased local convection and increased Atlantic westerly moisture transport and rainfall over the coasts of Angola and Namibia (Rouault et al., 2003; Reason and Smart, 2015). During MA, the relationship between DSF/MWDF and SST averaged over the SE Atlantic was consistent with these observations since positive SST anomalies were associated with decreased (increased) DSF (MWDF) over the southwestern Angola and northwestern Namibia (the coast of Angola). Since warm events develop through summer (Florenchie et al., 2004), they may impact rainfall over coastal Angola and Namibia during ON and DJF as well, as suggested by positive correlations with seasonal rainfall (not shown) and nega-

tive (positive) correlations with DSF (MWDF) over coastal Angola and Namibia.

Regressions with various atmospheric fields and SST point to the potential mechanisms associated with change in DSF and MWD patterns. For region 1, in Fig. 12, regression patterns with 500 hPa geopotential height are reminiscent of pressure anomalies associated with the SAM and indicate that a high occurrence of dry spells (moderate wet days) tends to coincide with negative (positive) SAM phases. This is consistent with what is known about SAM impacts on southern African rainfall. The southward shift (positive phase) of the southern hemisphere westerlies is associated with increased precipitation over the region (Gillett et al., 2006). DSF (MWDF) also has a positive (negative) relationship with geopotential height at 500 hPa over the Botswana High region. This midtropospheric anticyclone has been shown to influence rainfall over southern Africa (Driver and Reason, 2017; Blamey et al., 2018). When intensified, subsidence associated the Botswana High inhibits cloud formation and results in dry conditions over many parts of southern Africa. Conversely, weak pressure anomalies in the Botswana high are associated with increased uplift and moisture advection from the SWIO over southern Africa (Driver and Reason, 2017). The relationship with omega at 500 hPa over the southern African interior is consistent with dry (wet) conditions over region 1 since omega values are indicative of relative subsidence and uplift. OLR values are indicative of convection and cloud cover and regressions suggest that trends in the occurrence of DSF and MWDF over region 1 are associated with changes in the occurrence of continental cloud bands over southern Africa.

SST regression patterns display a strong ENSO-like signal in the tropical Pacific. This is consistent with the rainfall anomalies known to be associated with ENSO since El Niño (La Niña) events tend to coincide with below (above) average rainfall over many parts of southern Africa (Nicholson and Kim, 1997; Reason and Jagadheesha, 2005). Region 1 DSF (MWDF) indeed is strongly positively (negatively) correlated with the Niño 3.4 index (Figs. 9c and 9d). Regressed SST also shows a relationship with SST events in the tropical SE Atlantic where warm events are associated with decreased DSF within the region. While these events are associated with rainfall anomalies mainly over the coast of Angola and Namibia, rainfall anomalies have been shown to sometimes extend to the interior of southern Africa when convergence between moist air from the SE Atlantic and Indian Ocean is intensified (Rouault et al., 2003). The increased occurrence of dry spells (wet days) is also associated with increased (decreased) westerly moisture flux from the South Atlantic.

Cool and dry air from the South Atlantic advected over southern Africa leads to drought conditions over region 1 and may prevent the penetration of easterly moisture fluxes from the southern Indian Ocean (Reason et al., 2006).

Over region 2, DSF (MWDF) is negatively (positively) associated with pressure anomalies in the the Mascarene High and MCT region. Both pressure systems have been shown to influence rainfall variability over southern Africa. A weaker Mascarene High transports less moisture from the South Indian Ocean towards southeastern Africa (Morioka et al., 2015; Xulu et al., 2020) whereas stronger MCT discourages the direct advection of warm moist air to the southern African mainland (Barimalala et al., 2018, 2020). OLR and omega regressions patterns extending from the interior of southern Africa southeastwards towards the SWIO are reminiscent of the SICZ. Relative uplift and convective activity occurring over this region are associated with the increased (decreased) occurrence of dry spells (wet days). These processes, along with enhanced easterly moisture flux from the southern Indian Ocean (Fig. 17a), are consistent with Barimalala et al. (2018) who showed that a weakened MCT and associated increased moisture flux from the Mascarene High result in a stronger SICZ and increased rainfall over southern Africa.

Regressed SST plots display a strong SIOD-like signal, suggesting that positive (negative) SIOD phases tend to be associated with high (low) MWDF and low (high) DSF over region 2. Indeed, SIOD index has a strong negative (positive) relationship with DSF (MWD) over region 2 (Figs. 10a and 10b). Positive SIOD phases have been shown to be associated with above average rainfall anomalies over many parts of southern Africa (Reason, 2001). Plots showing correlations with climate indices and regressed SST suggest that the relationship between DSF/MWDF over region 2 and SIOD is stronger than that with ENSO. Mosase and Ahiablame (2018) found that ENSO did not impact significantly on rainfall variability over the Limpopo River Basin, which region 2 forms a part of. Regressions between DSF/MWDF and SST in the eastern and western Pacific are reminiscent of a weak ENSO Modoki marked by SST anomalies of the same sign on either side of the Pacific basin (Ashok et al., 2007). El Niño Modokis have been shown to be associated with below average rainfall anomalies over parts of southern Africa (Ratnam et al., 2014). The negative relationship between DSF and SST in the Pacific is consistent with these observations.

6 Summary

This study found that two strong gradients in DSF exist over southern Africa during austral summer. One is diagonal, covering southwestern Angola, Namibia and western South Africa and the other meridional, lying across 20-24°S. These gradients were present during ON and MA as well, however, they were less clearly defined and weaker. Topographic influences were observed over eastern South Africa, roughly along the windward slopes of the Drakensberg, the central and northern peaks of the Madagascan highlands, the peaks of the Chimanimani mountain range and east of the Mulalnje massif, areas that had relatively higher MWDF and lower DSF.

A preferred region of dry spell occurrence was found lying roughly across 22-24°S, where more than half of the austral summer season was frequently made up dry spells. This is the drought corridor which was first described as a preferred region of high dry spell frequencies, lying across 20-25°S by Usman and Reason (2004). In this study it was found along a more tightly defined area. Additionally, a core not present in Usman and Reason (2004) was observed over the LRV where 85-100% of the 38 summers were dry for half the season. This observation is likely due to the higher resolution of the data used in this study. During MA, a region analogous to the drought corridor where seasons are frequently made up of 6 or more dry spells was present roughly across 18-25°S with a core in the central LRV where 100% of seasons were dry for half the season. These regions are highly susceptible to multi-year droughts and comparable with the arid and semi-arid western margins of southern Africa. For this reason they unsuitable for rainfed agriculture. Intensity-frequency maps of moderate wet day frequencies show that subtropical southern Africa infrequently had at least 10 wet days during ON and MA and 20 during DJF. This suggests that rainfall over the region often does not meet water requirements for agriculture and over-reliance on rainfall for food production is risky.

During ON increasing trends in DSF and a combination of increasing dry spell and weak increasing wet day trends over central South Africa, the southern portion of the diagonal DSF gradient suggest that early summer drying has taken place. This may affect the planting season of maize if trends persist since this is typically the onset season. By contrast, decreasing trends in DSF were found to have taken place roughly over the diagonal gradient over northern Namibia, western Botswana and central South Africa during DJF. These point

towards a weakening and westward shift in the gradient that has taken place. A weakening of part of the meridional gradient has also taken place as is suggested by decreasing (increasing) DSF (MWDF) trends occurring over eastern Botswana and western Zimbabwe during DJF. Increasing MWDF trends during DJF have also taken place over central Angola and central and eastern South Africa, important agricultural areas within southern Africa. Austral summer trends suggest that a tendency toward more consistent rainfall has taken place. If these continue, land use may change over the regions mentioned above.

Various modes of climate variability were shown to be significantly associated with DSF and MWDF over southern Africa. ENSO had a positive (negative) relationship with DSF (MWDF) over southern Africa during all three seasons however the relationship was most robust during DJF. The SIOD was observed to have a positive (negative) relationship with DSF (MWDF) over southeastern Africa whereas SAM was negatively correlated with DSF over South Africa during austral summer. For region 1, located in the South African part of the diagonal DSF gradient, regressions suggest that trends in DSF and MWDF were associated with changes in the Botswana High, SAM, ENSO and SST in the tropical SE Atlantic during DJF. Trends over region 2, which forms part of the meridional gradient, were shown to be associated with changes in the Mascarene High, MCT, SIOD and SST in the eastern and western Pacific.

The analysis of dry spells and moderate wet day frequencies over southern Africa shows that large parts of southern Africa are not suitable for rainfed agriculture despite the heavy reliance on rainfall for farming within the region. Innovative strategies are therefore required to build resilience and recover from prolonged dry periods. Recent trends point towards early summer drying and more consistent rainfall during the main rainy season. If trends follow in the same trajectory, collaboration between stakeholders in the agricultural sector is required to develop solutions to deal with the challenges associated with shifts in rainfall patterns.

This study sets a foundation by identifying potential mechanisms for recent trends but does not directly attribute change to the discussed circulations. Further work is required to investigate the spatial and temporal changes in circulation features, weather systems and climate modes associated with change.

Appendix A1

Seasonal rainfall totals

As seasonal totals are the aggregate of wet and dry events during the season, seasonal total climatologies and coefficients of seasonal variation in Fig. A1 provide a background for the analysis of the occurrence of dry spells and moderate wet days over southern Africa.

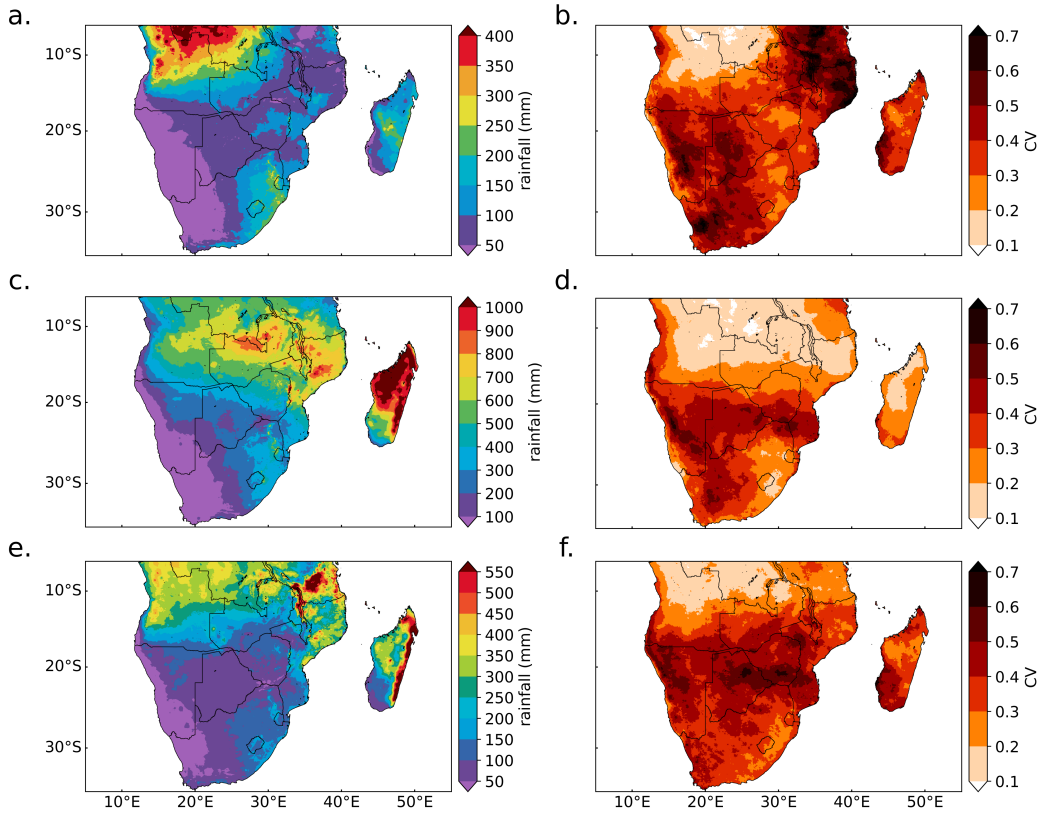

Figure A1: Mean seasonal rainfall totals during a. ON, c. DJF and e. MA and mean coefficients of variation of seasonal rainfall totals during b. ON, d. DJF and f. MA averaged over the period 1981/82-2018/19.

Over the southern African mainland, relatively high rainfall values (>250 mm during ON and MA, >600 mm during DJF) are found mostly over regions of tropical convergence. These areas include northern Angola-eastern DR Congo during ON, 6- 19°S during DJF and roughly 6- 15°S during MA, and roughly correspond to the north-south movement and change in latitudinal span of the tropical rainbelt outlined by Nicholson (2018). The increase in the area of high rainfall values from ON through DJF matches the southward shift

in the position of the rainbelt and the decrease during MA, the slight northward movement and decrease in the width of rainbelt.

An east-west gradient in seasonal rainfall totals is apparent during all three seasons. Minimum values ($<$50 mm during ON and MA, $<$100 mm during DJF) are observed over the arid and semi arid western margins of the southern Africa. The topographic influence of the Drakensberg mountain range is observed over eastern South Africa where rainfall values are relatively higher through all the seasons. A unique feature of the climatologies shown in Fig. A1 over subtropical southern Africa during ON and MA is the expansion of the region low seasonal totals (0-100 mm) in the western region eastward towards Mozambique. This feature is present roughly across 20-24°S and 18-24°S, respectively. During DJF, relatively low values (100-200 mm) are observed over central Botswana and the central LRV.

Maps of the coefficient of variation (CV) of mean seasonal southern African rainfall are shown in Figs. A1b, d and f. Higher CV values are indicative of greater interannual rainfall variability. Generally, the tropical regions of higher seasonal rainfall outlined above correspond to regions of low CV values ($<$0.2). During ON, the region of low variability is contrasted by that of high CVs observed over Tanzania, Malawi and northern Mozambique, where values exceed 0.5. Subtropical western and central southern Africa also experience considerable rainfall variability ($>$0.4). During DJF, higher values ($>$0.4) are found along western southern Africa and across 20-24°S, with relative maximums in the LRB. The latter region is found lying across 20-22°S in Botswana, Zimbabwe and Mozambique during MA.

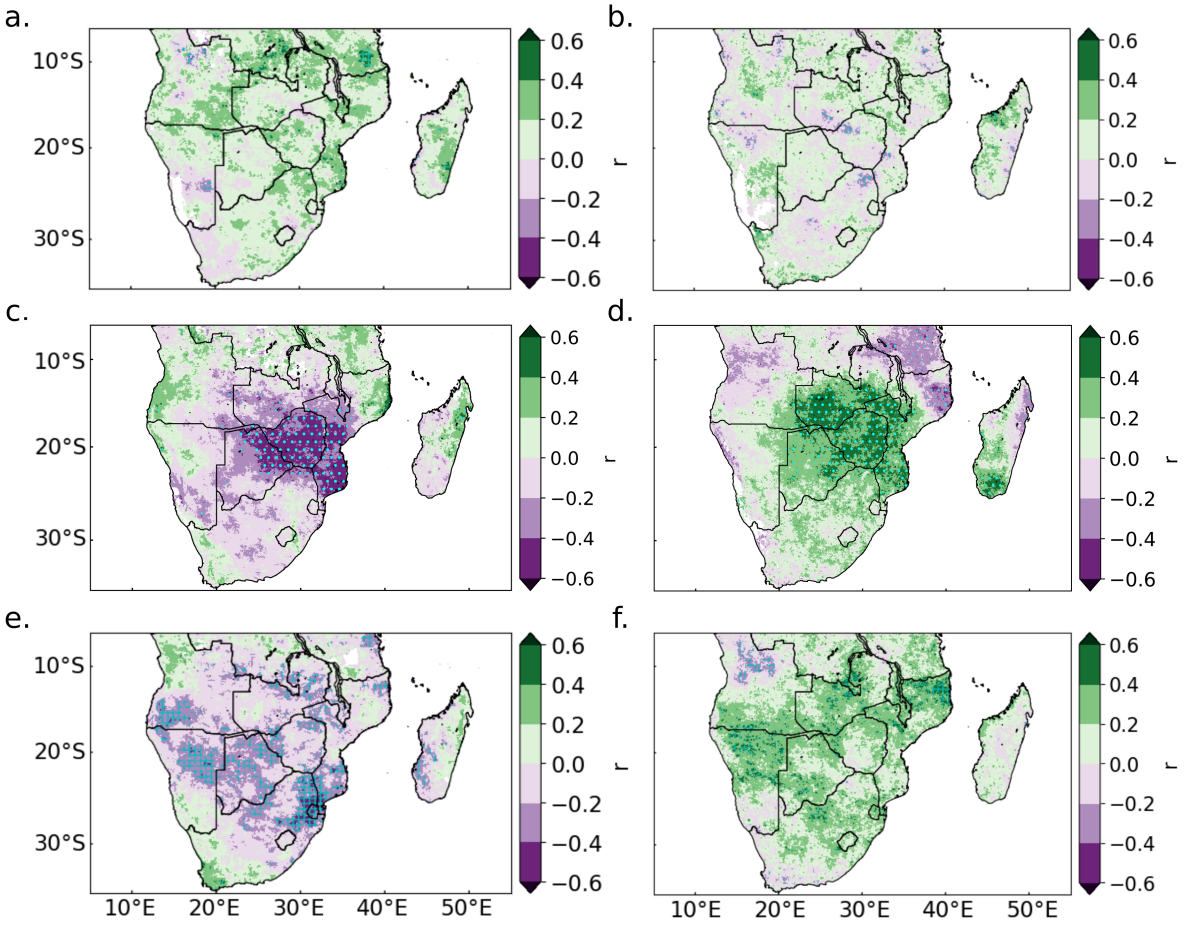

Figure A2: Correlation coefficients between the SIOD index and dry spell frequencies during a. ON, c. DJF and e. MA, and with moderate wet day frequencies during b. ON , d. DJF and f. MA. Hatching denotes areas of significant correlations (95% confidence level) calculated over the period 1981/1982 – 2018/2019.

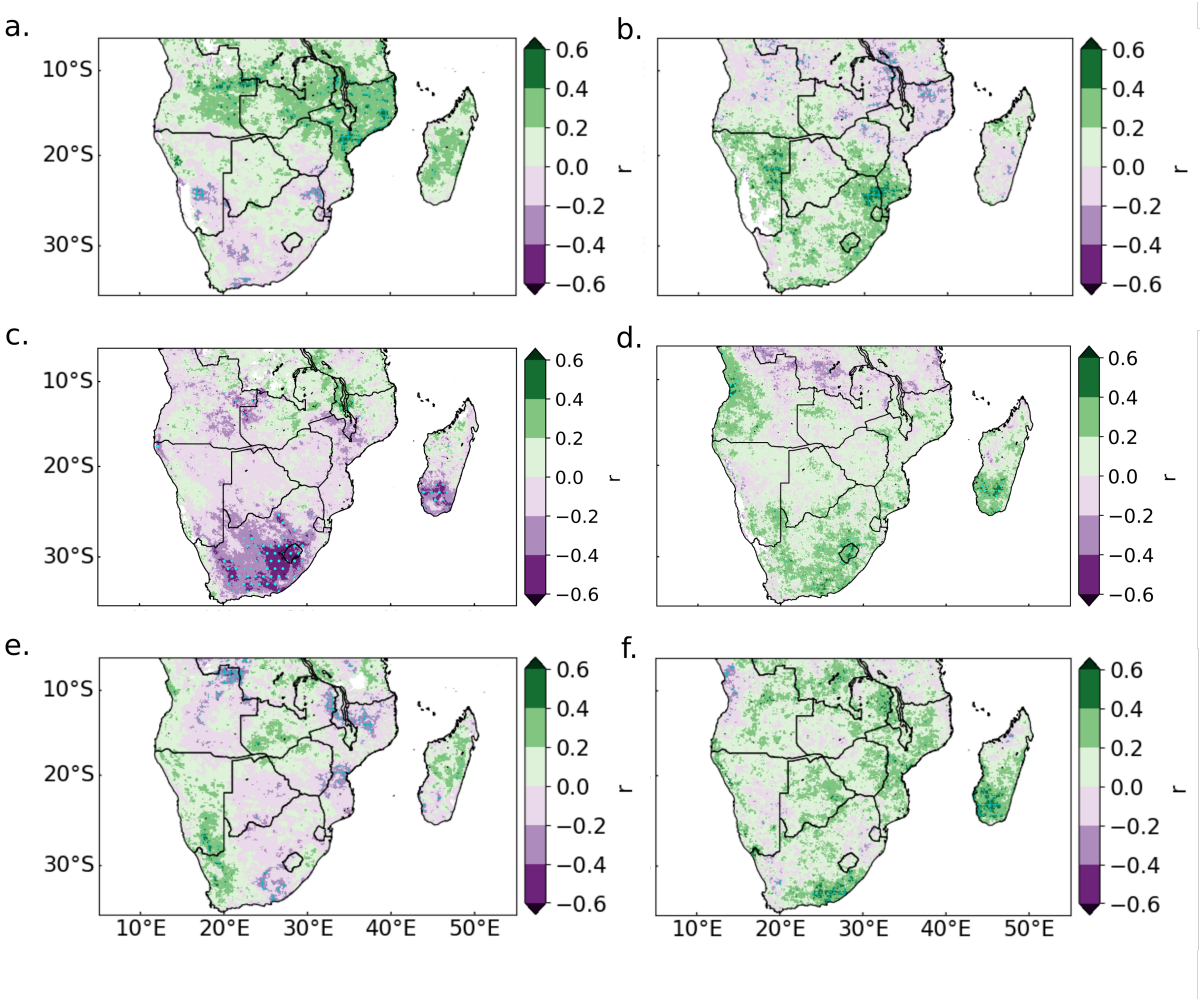

Figure A3: Correlation coefficients between the SAM index and dry spell frequencies during a. ON, c. DJF and e. MA, and with moderate wet day frequencies during b. ON , d. DJF and f. MA. Hatching denotes areas of significant correlations (95% confidence level) calculated over the period 1981/1982 – 2018/2019.

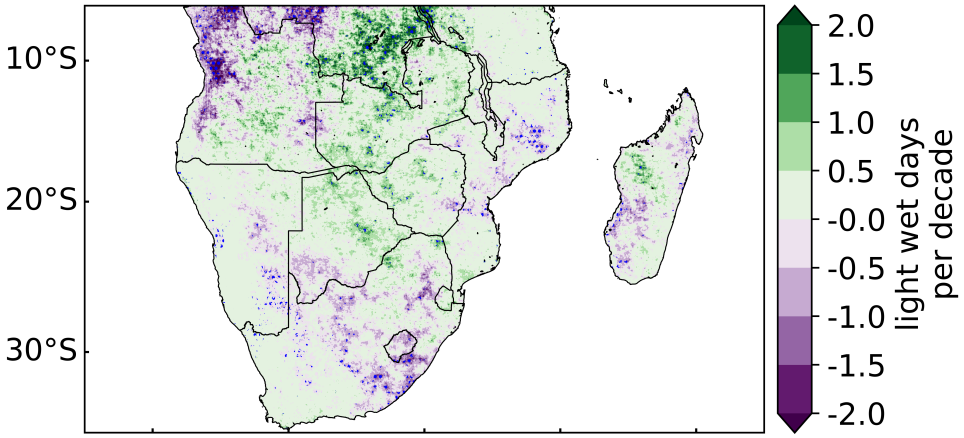

Figure A4: Trends in light wet days (2-9 mm) during ON. Hatching denotes areas of significant trends (5% level) calculated over the period 1981/1982–2018/2019.

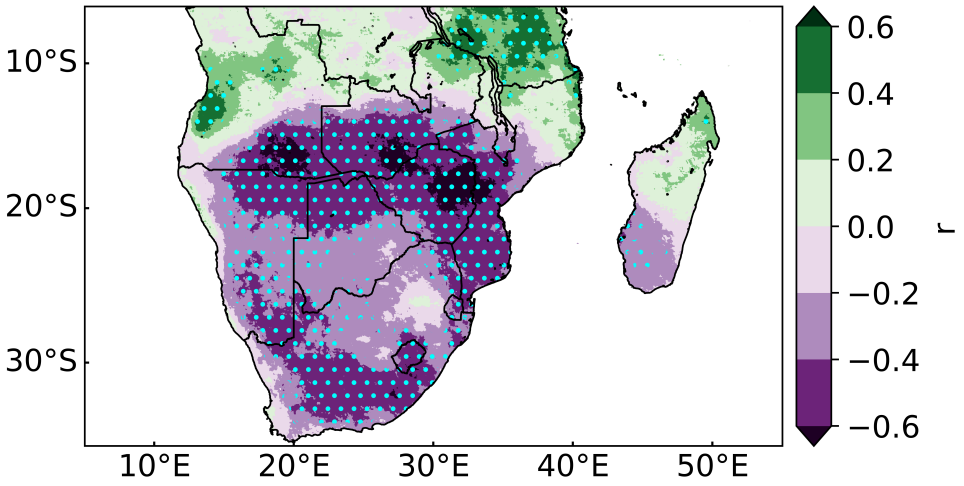

Figure A5: Correlation coefficients between the Niño 3.4 index and seasonal rainfall totals during DJF Hatching denotes areas of significant trends (5% level) calculated over the period 1981/1982–2018/2019.

References

Ashok, K., Behera, S. K., Rao, S. A., Weng, H. & Yamagata, T. 2007. El Niño Modoki and its possible teleconnection. *Journal of Geophysical Research: Oceans*, 112(C11).

Ashouri, H., Hsu, K.-L., Sorooshian, S., Braithwaite, D. K., Knapp, K. R., Cecil, L. D. et al. 2015. PERSIANN-CDR: Daily precipitation climate data record from multisatellite observations for hydrological and climate studies. *Bulletin of the American Meteorological Society*, 96(1):69–83.

Barimalala, R., Desbiolles, F., Blamey, R. C. & Reason, C. J. C. 2018. Madagascar influence on the South Indian Ocean convergence zone, the Mozambique Channel Trough and southern African rainfall. *Geophysical Research Letters*, 45(20):11–380.

Barimalala, R., Blamey, R. C., Desbiolles, F. & Reason, C. J. C. 2020. Variability in the Mozambique Channel Trough and impacts on southeast African rainfall. *Journal of Climate*, 33(2):749–765.

Behera, S. K. & Yamagata, T. 2001. Subtropical SST dipole events in the southern Indian Ocean. *Geophysical Research Letters*, 28(2):327–330.

Blamey, R. C., Kolusu, S. R., Mahlalela, P., Todd, M. C. & Reason, C. J. C. 2018. The role of regional circulation features in regulating El Niño climate impacts over southern Africa: A comparison of the 2015/2016 drought with previous events. *International Journal of Climatology*, 38(11):4276–4295.

Chen, H. C. & Jin, F. F. 2020. Fundamental Behavior of ENSO Phase Locking. *Journal of Climate*, 33(5):1953–1968.

Chikoore, H. & Jury, M. R. 2010. Intraseasonal variability of satellite-derived rainfall and vegetation over Southern Africa. *Earth Interactions*, 14(3):1–26.

Cloete, S. & Olivier, J. 2010. South African sheep and wool industries. *International sheep and wool Handbook*, 95–104.

Collier, A. B. & Hughes, A. R. W. 2011. Lightning and the African ITCZ. *Journal of Atmospheric and Solar-Terrestrial Physics*, 73(16):2392–2398.

Conceição, P., Levine, S., Lipton, M. & Warren-Rodríguez, A. 2016. Toward a food secure future: Ensuring food security for sustainable human development in Sub-Saharan Africa. *Food Policy*, 60:1–9.

Cook, C., Reason, C. J. C. & Hewitson, B. C. 2004. Wet and dry spells within particularly wet and dry summers in the South African summer rainfall region. *Climate Research*, 26(1):17–31.

Cook, K. H. 2000. The South Indian Convergence Zone and interannual rainfall variability over southern Africa. *Journal of Climate*, 13(21):3789–3804.

Crétat, J., Pohl, B., Dieppois, B., Berthou, S. & Pergaud, J. 2019. The Angola Low: relationship with southern African rainfall and ENSO. *Climate Dynamics*, 52(34):1783–1803.

Dedekind, Z., Engelbrecht, F. A. & Van Der Merwe, J. 2016. Model simulations of rainfall over southern Africa and its eastern escarpment. *Water SA*, 42(1):129–143.

Dee, D. P., Uppala, S. M., Simmons, A., Berrisford, P., Poli, P., Kobayashi, S. et al. 2011. The ERA-Interim reanalysis: Configuration and performance of the data assimilation system. *Quarterly Journal of the Royal Meteorological Society*, 137(656):553–597.

Driver, P. & Reason, C. J. C. 2017. Variability in the Botswana High and its relationships with rainfall and temperature characteristics over southern Africa. *International Journal of Climatology*, 37:570–581.

Dunning, C. M., Black, E. C. & Allan, R. P. 2016. The onset and cessation of seasonal rainfall over Africa. *Journal of Geophysical Research: Atmospheres*, 121(19):11–405.

Dunning, C. M., Black, E. C. & Allan, R. P. 2018. Later wet seasons with more intense rainfall over Africa under future climate change. *Journal of Climate*, 31(23):9719–9738.

Fauchereau, N., Trzaska, S., Rouault, M. & Richard, Y. 2003. Rainfall variability and changes in southern Africa during the 20th century in the global warming context. *Natural Hazards*, 29(2):139–154.

Fauchereau, N., Pohl, B., Reason, C. J. C., Rouault, M. & Richard, Y. 2009. Recurrent daily OLR patterns in the southern Africa/southwest Indian ocean region, implications for South African rainfall and teleconnections. *Climate Dynamics*, 32(4):575–591.

Ferreira, R. N. & Schubert, W. H. 1997. Barotropic aspects of ITCZ breakdown. *Journal of the Atmospheric Sciences*, 54(2):261–285.

Florenchie, P., Lutjeharms, J. R., Reason, C. J. C., Masson, S. & Rouault, M. 2003. The source of Benguela Niños in the south Atlantic Ocean. *Geophysical Research Letters*, 30(10).

Florenchie, P., Reason, C. J. C., Lutjeharms, J., Rouault, M., Roy, C. & Masson, S. 2004. Evolution of interannual warm and cold events in the southeast Atlantic Ocean. *Journal of Climate*, 17(12):2318–2334.

Funk, C., Peterson, P., Landsfeld, M., Pedreros, D., Verdin, J., Shukla, S. et al. 2015. The climate hazards infrared precipitation with stations—a new environmental record for monitoring extremes. *Scientific Data*, 2(1):1–21.

Gillett, N. P., Kell, T. D. & Jones, P. 2006. Regional climate impacts of the Southern Annular Mode. *Geophysical Research Letters*, 33(23).

Goddard, L. & Graham, E. 1999. Importance of the Indian Ocean for simulating rainfall anomalies over eastern and southern Africa. *Journal of Geophysical Research*, 104(D16):19099–19116.

Grodsky, S. A. & Carton, J. A. 2003. The intertropical convergence zone in the south Atlantic and the equatorial cold tongue. *Journal of Climate*, 16(4):723–733.

Hachigonta, S. & Reason, C. J. C. 2006. Interannual variability in dry and wet spell characteristics over Zambia. *Climate Research*, 32(1):49–62.

Hachigonta, S., Reason, C. J. C. & Tadross, M. 2008. An analysis of onset date and rainy season duration over Zambia. *Theoretical and Applied Climatology*, 91(1-4):229– 243.

Ham, Y. G., Kug, J. S., Kim, D., Kim, Y. H. & Kim, D. H. 2013. What controls phase-locking of ENSO to boreal winter in coupled GCMs? *Climate Dynamics*, 40(56):1551–1568.

Harrison, M. 1984. A generalized classification of South African summer rainbearing synoptic systems. *Journal of Climatology*, 4(5):547–560.

Hart, N. C. G., Reason, C. J. C. & Fauchereau, N. 2010. Tropical–extratropical interactions over southern Africa: Three cases of heavy summer season rainfall. *Monthly Weather Review*, 138(7):2608–2623.

Hart, N. C. G., Reason, C. J. C. & Fauchereau, N. 2013. Cloud bands over southern Africa: seasonality, contribution to rainfall variability and modulation by the MJO. *Climate Dynamics*, 41(5-6):1199–1212.

Hart, N. C. G., Washington, R. & Reason, C. J. C. 2018. On the likelihood of Tropical–extratropical cloud bands in the South Indian Convergence Zone during ENSO Events. *Journal of Climate*, 31(7):2797–2817.

Hermes, J. C. & Reason, C. J. C. 2005. Ocean model diagnosis of interannual coevolving SST variability in the south Indian and south Atlantic Oceans. *Journal of Climate*, 18(15):2864–2882.

Hersbach, H., Bell, B., Berrisford, P., Hirahara, S., Horányi, A., MuñozSabater J. et al. 2020. The ERA5 global reanalysis. *Quarterly Journal of the Royal Meteorological Society*, 146(730):1999–2049.

Hoerling, M. P., Kumar, A. & Xu, T. 2001. Robustness of the nonlinear climate response to ENSO's extreme phases. *Journal of Climate*, 14(6):1277–1293.

Hoffmann, L., Günther, G., Li, D., Stein, O., Wu, X., Griessbach, S. et al. 2019. From ERA-Interim to ERA5: the considerable impact of ECMWF's next-generation reanalysis on Lagrangian transport simulations. *Atmospheric Chemistry & Physics*, 19(5):3097–3124.

Howard, E. & Washington, R. 2018. Characterizing the synoptic expression of the Angola low. *Journal of Climate*, 31(17):7147–7165.

Huang, J., Ji, M., Xie, Y., Wang, S., He, Y. & Ran, J. 2016. Global semi-arid climate change over last 60 years. *Climate Dynamics*, 46(3-4):1131–1150.

Huffman, G. J., Bolvin, D. T., Nelkin, E. J., Wolff, D. B., Adler, R. F., Gu, G. et al. 2007. The TRMM multisatellite precipitation analysis (TMPA): Quasiglobal, multiyear, combined-sensor precipitation estimates at fine scales. *Journal of Hydrometeorology*, 8(1):38–55.

IPCC, 2013. Climate Change 2013: *The Physical Science Basis. Contribution of Working Group I to the Fifth Assessment Report of the Intergovernmental Panel on Climate Change*. Cambridge: Cambridge University Press.

Janowiak, J. E. 1988. An investigation of interannual rainfall variability in Africa. *Journal of Climate*, 1(3):240–255.

Jury, M. R., Parker, B., Raholijao, N. & Nassor, A. 1995. Variability of summer rainfall over Madagascar: climatic determinants at interannual scales. *International Journal of Climatology*, 15(12):1323–1332.

Kanamitsu, M., Ebisuzaki, W., Woollen, J., Yang, S. K., Hnilo, J., Fiorino, M. & Potter, G. 2002. NCEP-DOE AMIP-II Reanalysis (R-2). *Bulletin of the American Meteorological Society*, 83(11):1631–1644.

Kendall, M. G. 1975. Rank Correlation Methods. London: Charles Griffin.

Kijazi, A. & Reason, C. J. C. 2005. Relationships between intraseasonal rainfall variability of coastal Tanzania and ENSO. *Theoretical and Applied Climatology*, 82(3-4):153–176.

Landman, W. A. & Beraki, A. 2012. Multi-model forecast skill for mid-summer rainfall over southern Africa. *International Journal of Climatology*, 32(2):303–314.

Lee, S. K., Mapes, B. E., Wang, C., Enfield, D. B. & Weaver, S. J. 2014. Springtime ENSO phase evolution and its relation to rainfall in the continental US. *Geophysical Research Letters*, 41(5):1673–1680.

Lipper, L., Thornton, P., Campbell, B. M., Baedeker, T., Braimoh, A., Bwalya, M. et al. 2014. Climate-smart agriculture for food security. *Nature Climate Change*, 4(12):1068–1072.

Lyon, B. & Mason, S. J. 2007. The 1997-98 summer rainfall season in southern Africa. Part I: Observations. *Journal of Climate*, 20(20):5134–5148.

Macron, C., Pohl, B., Richard, Y. & Bessafi, M. 2014. How do tropical temperate troughs form and develop over southern Africa? *Journal of Climate*, 27(4):1633–1647.

Mahlalela, P., Blamey, R., Hart, N. & Reason, C. 2020. Drought in the Eastern Cape region of South Africa and trends in rainfall characteristics. *Climate Dynamics*, 55(9):2743–2759.

Malherbe, J., Landman, W. A. & Engelbrecht, F. A. 2014. The bi-decadal rainfall cycle, Southern Annular Mode and tropical cyclones over the Limpopo River Basin, southern Africa. *Climate Dynamics*, 42(11-12):3121–3138.

Mangani, R., Tesfamariam, E. H., Engelbrecht, C. J., Bellocchi, G., Hassen, A. & Mangani, T. 2019. Potential impacts of extreme weather events in main maize (Zea mays L.) producing areas of South Africa under rainfed conditions. *Regional Environmental Change*, 19(5):1441–1452.

Mann, H. B. 1945. Nonparametric tests against trend. *Econometrica: Journal of the econometric society*, 245–259.

Mapande, A. T. & Reason, C. J. C. 2005. Links between rainfall variability on intraseasonal and interannual scales over western Tanzania and regional circulation and SST patterns. *Meteorology and Atmospheric Physics*, 89(14):215–234.

Marshall, G. J. 2003. Trends in the Southern Annular Mode from observations and reanalyses. *Journal of Climate*, 16(24):4134–4143.

Meque, A. & Abiodun, B. J. 2015. Simulating the link between ENSO and summer drought in southern Africa using regional climate models. *Climate Dynamics*, 44(78):1881–1900.

Moore, A., Blenkinsop, T. & Cotterill, F. 2009. Southern African topography and erosion history: Plumes or plate tectonics? *Terra Nova*, 21(4):310–315.

Morioka, Y., Tozuka, T. & Yamagata, T. 2011. On the growth and decay of the subtropical dipole mode in the South Atlantic. *Journal of Climate*, 24(21):5538–5554.

Morioka, Y., Tozuka, T., Masson, S., Terray, P., Luo, J.-J. & Yamagata, T. 2012. Subtropical dipole modes simulated in a coupled general circulation model. *Journal of Climate*, 25(12):4029–4047.

Morioka, Y., Takaya, K., Behera, S. K. & Masumoto, Y. 2015. Local SST impacts on the summertime Mascarene high variability. *Journal of Climate*, 28(2):678–694.

Mosase, E. & Ahiablame, L. 2018. Rainfall and temperature in the Limpopo river basin, Southern Africa: means, variations, and trends from 1979 to 2013. *Water*, 10(4):364.

Mulenga, H. M., Rouault, M. & Reason, C. J. C. 2003. Dry summers over northeastern South Africa and associated circulation anomalies. *Climate Research*, 25(1):29–41

Munday, C. & Washington, R. 2017. Circulation controls on southern African precipitation in coupled models: The role of the Angola low. *Journal of Geophysical Research: Atmospheres*, 122(2):861–877.

Munday, C. & Washington, R. 2019. Controls on the diversity in climate model projections of early summer drying over southern Africa. *Journal of Climate*, 32(12):3707– 3725.

Munodawafa, A. 2012. The effect of rainfall characteristics and tillage on sheet erosion and maize grain yield in semiarid conditions and granitic sandy soils of Zimbabwe. *Applied and Environmental Soil Science*, 2012.

Mutai, C. C. & Ward, M. N. 2000. East African rainfall and the tropical circulation/convection on intraseasonal to interannual timescales. *Journal of Climate*, 13(22):3915–3939.

Nicholson, S. E. & Entekhabi, D. 1987. Rainfall variability in equatorial and southern Africa: Relationships with sea surface temperatures along the southwestern coast of Africa. *Journal of Climate and Applied Meteorology*, 26(5):561–578.

Muthoni, F. K., Odongo, V. O., Ochieng, J., Mugalavai, E. M., Mourice, S. K., Hoesche-Zeledon, I. et al. 2019. Long-term spatial temporal trends and variability of rainfall over Eastern and Southern Africa. *Theoretical and Applied Climatology*, 137(3-4):1869–1882.

Ndarana, T., Bopape, M.-J., Waugh, D. & Dyson, L. 2018. The influence of the lower stratosphere on ridging Atlantic Ocean anticyclones over South Africa. *Journal of Climate*, 31(15):6175–6187.

Nicholson, S. E. & Kim, J. 1997. The relationship of the El Niño–Southern oscillation to African rainfall. *International Journal of Climatology*, 17(2):117–135.

Nicholson, S. E. 2000. The nature of rainfall variability over Africa on time scales of decades to millenia. *Global and Planetary Change*, 26(1-3):137–158.

Nicholson, S. E. 2018. The ITCZ and the seasonal cycle over equatorial Africa. *Bulletin of the American Meteorological Society*, 99(2):337–348.

Phillips, J., Cane, M. & Rosenzweig, C. 1998. ENSO, seasonal rainfall patterns and simulated maize yield variability in Zimbabwe. *Agricultural and Forest Meteorology*, 90(1-2):39–50.

Pohl, B., Macron, C. & Monerie, P. A. 2017. Fewer rainy days and more extreme rainfall by the end of the century in Southern Africa. *Scientific Reports*, 7(1):1–7.

Raes, D., Sithole, A., Makarau, A. & Milford, J. 2004. Evaluation of first planting dates recommended by criteria currently used in Zimbabwe. *Agricultural and Forest Meteorology*, 125(3-4):177–185.

Randriamahefasoa, T. S. M. & Reason, C. J. C. 2017. Interannual variability of rainfall characteristics over southwestern Madagascar. *Theoretical and Applied Climatology*, 128(1-2):421–437.

Rapolaki, R. S., Blamey, R. C., Hermes, J. C. & Reason, C. J. C. 2019. A classification of synoptic weather patterns linked to extreme rainfall over the Limpopo River Basin in southern Africa. *Climate Dynamics,* 53(34):2265–2279.

Rapolaki, R. S., Blamey, R. C., Hermes, J. C. & Reason, C. J. C. 2020. Moisture sources associated with heavy rainfall over the Limpopo River Basin, southern Africa. *Climate Dynamics*, 55(5):1473–1487.

Ratna, S. B., Behera, S., Ratnam, J. V., Takahashi, K. & Yamagata, T. 2013. An index for tropical temperate troughs over southern Africa. *Climate Dynamics*, 41(2):421–441.

Ratnam, J., Behera, S., Masumoto, Y. & Yamagata, T. 2014. Remote effects of El Niño and Modoki events on the austral summer precipitation of southern Africa. *Journal of Climate*, 27(10):3802–3815.

Rayner, N., Parker, D. E., Horton, E., Folland, C. K., Alexander, L. V., Rowell, D. et al. 2003. Global analyses of sea surface temperature, sea ice, and night marine air temperature since the late nineteenth century. *Journal of Geophysical Research: Atmospheres*, 108(D14).

Reason, C. J. C., Allan, R. J., Lindesay, J. A. & Ansell, T. J. 2000. ENSO and climatic signals across the Indian Ocean basin in the global context: Part I, interannual composite patterns. *International Journal of Climatology*, 20(11):1285–1327.

Reason, C. J. C. 2001. Subtropical Indian Ocean SST dipole events and southern African rainfall. *Geophysical Research Letters*, 28(11):2225–2227.

Reason, C. J. C. 2002. Sensitivity of the southern African circulation to dipole sea surface temperature patterns in the south Indian Ocean. *International Journal of Climatology*, 22(4):377–393.

Reason, C. J. C. & Rouault, M. 2002. ENSO-like decadal variability and South African rainfall. *Geophysical Research Letters*, 29(13):16–1.

Reason, C. J. C., Hachigonta, S. & Phaladi, R. F. 2005. Interannual variability in rainy season characteristics over the Limpopo region of southern Africa. International Journal of Climatology, 25(14):1835–1853.

Reason, C. J. C. & Jagadheesha, D. 2005. A model investigation of recent ENSO impacts over southern Africa. *Meteorology and Atmospheric Physics*, 89(1-4):181–205.

Reason, C. J. C., Landman, W. & Tennant, W. 2006. Seasonal to decadal prediction of southern African climate and its links with variability of the Atlantic Ocean. *Bulletin of the American Meteorological Society*, 87(7):941–956.

Reason, C. J. C. & Smart, S. 2015. Tropical south east Atlantic warm events and associated rainfall anomalies over southern Africa. *Frontiers in Environmental Science*, 3(24):1-11.

Reason, C. J. C. 2016. The Bolivian, Botswana, and Bilybara Highs and southern Hemisphere drought/floods. *Geophysical Research Letters*, 43(3):1280–1286.

Reason, C. J. C. 2017. Climate of southern Africa. In *Oxford Research Encyclopedia of Climate Science*. Oxford University Press.

ReliefWeb 2015. Southern Africa: Food Insecurity – 2015-2017. Available: https://reliefweb.int/disaster/dr-2015-000137-mwi. [2020, October 24].

ReliefWeb 2017. Southern Africa: Floods - Jan 2017. Available: https://reliefweb.int/disaster/ fl-2017-000012-moz. [2020, October 24].

ReliefWeb 2018. Southern Africa: Drought - 2018-2020. Available: https://reliefweb.int/disaster/ dr-2018-000429-zwe. [2020, October 24].

Reynolds, R. W., Rayner, N. A., Smith, T. M., Stokes, D. C. & Wang, W. 2002. An improved in situ and satellite SST analysis for climate. *Journal of Climate*, 15(13):1609– 1625.

Rouault, M., Florenchie, P., Fauchereau, N. & Reason, C. J. C. 2003. South East tropical Atlantic warm events and southern African rainfall. *Geophysical Research Letters*, 30(5).

Rouault, M., Servain, J., Reason, C. J. C, Bourlès, B., Rouault, M. & Fauchereau, N. 2009. Extension of PIRATA in the tropical South-East Atlantic: an initial one-year experiment. *African Journal of Marine Science*, 31(1):63–71.

Schneider, T., Bischoff, T. & Haug, G. H. 2014. Migrations and dynamics of the intertropical convergence zone. *Nature*, 513(7516):45.

Sen, P. K. (1968). Estimates of the regression coefficient based on Kendall's tau. *Journal of the American Statistical Association*, 63(324):1379–1389.

Shannon, L., Boyd, A., Brundrit, G. & Taunton-Clark, J. 1986. On the existence of an El Niño-type phenomenon in the Benguela system. Journal of Marine Research, 44(3):495–520.

Shukla, S., Funk, C., Peterson, P., McNally, A., Dinku, T., Barbosa, H. et al. 2017. The Climate Hazards group InfraRed Precipitation with Stations

(CHIRPS) dataset and its applications in drought risk management. In *EGU General Assembly Conference Abstracts*.

Steenwerth, K. L., Hodson, A. K., Bloom, A. J., Carter, M. R., Cattaneo, A., Chartres, C. J. et al. 2014. Climate-smart agriculture global research agenda: scientific basis for action. *Agriculture & Food Security*, 3(1):11.

Sullivan, A., Mwamakamba, S., Mumba, A., Hachigonta, S. & Sibanda, L. M. 2012. Climate smart agriculture: More than technologies are needed to move smallholder farmers toward resilient and sustainable livelihoods. *FANRPAN Policy Brief*, 2(13).

Suzuki, R., Behera, S. K., Iizuka, S. & Yamagata, T. 2004. Indian Ocean subtropical dipole simulated using a coupled general circulation model. *Journal of Geophysical Research: Oceans*, 109(C9).

Tadross, M. A., Hewitson, B. C. & Usman, M. T. 2005. The interannual variability of the onset of the maize growing season over South Africa and Zimbabwe. *Journal of Climate*, 18(16):3356–3372.

Tadross, M., Suarez, P., Lotsch, A., Hachigonta, S., Mdoka, M., Unganai, L. et al. 2007. Changes in growing-season rainfall characteristics and downscaled scenarios of change over southern Africa: implications for growing maize. In *IPCC regional Expert Meeting on Regional Impacts, Adaptation, Vulnerability, and Mitigation, Nadi, Fiji*, 193–204.

Tadross, M., Suarez, P., Lotsch, A., Hachigonta, S., Mdoka, M., Unganai, L. et al. 2009. Growing-season rainfall and scenarios of future change in southeast Africa: implications for cultivating maize. *Climate Research*, 40(2-3):147–161.

Taljaard, J. J. 1986. Change of rainfall distribution and circulation patterns over southern Africa in summer. *Journal of Climatology*, 6(6):579–592.

Tennant, W. J. & Hewitson, B. C. 2002. Intra-seasonal rainfall characteristics and their importance to the seasonal prediction problem. *International Journal of Climatology*, 22(9):1033–1048.

Theil, H. 1950. A rank-invariant method of linear and polynominal regression analysis (Parts 1-3). In *Proceedings of the Royal Netherlands Academy of Sciences*, 53: Part I, 386-392, Part II, 521-525, Part III, 1397-1412

Thornton, P. K., Ericksen, P. J., Herrero, M. & Challinor, A. J. 2014. Climate variability and vulnerability to climate change: a review. *Global Change Biology*, 20(11):3313– 3328.

Todd, M. & Washington, R. 1999. Circulation anomalies associated with tropical temperate troughs in southern Africa and the south west Indian Ocean. *Climate Dynamics*, 15(12):937–951.

Tyson, P. D. & Preston-Whyte, R. A. 2000. *The Weather and Climate of Southern Africa*. 2nd ed. Oxford University Press.

Tyson, P., Cooper, G. R. J. & McCarthy, T. 2002. Millennial to multi-decadal variability in the climate of southern Africa. *International Journal of Climatology*, 22(9):1105–1117.

Usman, M. T. & Reason, C. J. C. 2004. Dry spell frequencies and their variability over southern Africa. *Climate Research*, 26(3):199–211.

Vigaud, N., Richard, Y., Rouault, M. & Fauchereau, N. 2009. Moisture transport between the south Atlantic Ocean and southern Africa: Relationships with summer rainfall and associated dynamics. *Climate Dynamics*, 32(1):113–123.

Wainer, I., Prado, L. F., Khodri, M. & Otto-Bliesner, B. 2014. Reconstruction of the South Atlantic Subtropical Dipole index for the past 12,000 years from surface temperature proxy. *Scientific Reports*, 4:5291.

Washington, R. & Preston, A. 2006. Extreme wet years over southern Africa: Role of Indian Ocean sea surface temperatures. *Journal of Geophysical Research*, 111(D15):D15104.

Weldon, D. & Reason, C. J. C. 2014. Variability of rainfall characteristics over the South Coast region of South Africa. *Theoretical and Applied Climatology*, 115(1):177–185.

Weltzin, J. F., Loik, M. E., Schwinning, S., Williams, D. G., Fay, P. A., Haddad, B. M. et al. 2003. Assessing the response of terrestrial ecosystems to potential changes in precipitation. *Bioscience*, 53(10):941–952.

Winsemius, H., Dutra, E., Engelbrecht, F., Archer Van Garderen, E., Wetterhall, F., Pappenberger, F. et al. 2014. The potential value of

seasonal forecasts in a changing climate in southern Africa. *Hydrology and Earth System Sciences*, 18(4):1525– 1538.

Wursten, B., Timberlake, J. & Darbyshire, I. 2017. The Chimanimani Mountains. *Kirkia*, 19(1):70–100.

Xulu, N. G., Chikoore, H., Bopape, M.-J. M. & Nethengwe, N. S. 2020. Climatology of the Mascarene High and its influence on weather and climate over southern Africa. *Climate*, 8(7):86.

Yan, Y. Y. 2005. Intertropical Convergence Zone (ITCZ), In: *Encyclopedia of World Climatology*. Springer, Dordrecht.

Ziervogel, G., Nyong, A., Osman, B., Conde, C., Cortés, S. & Downing, T. 2006. Climate variability and change: Implications for household food security. *Assessment of Impacts and Adaptations to Climate Change (AIACC) Working Papers*, 6.